

An Overview of Particle Methods for Random Finite Set Models

Branko Ristic^{a,*}, Michael Beard^b, Claudio Fantacci^c

^a*RMIT University, Australia*

^b*Curtin University, Australia*

^c*Università di Firenze, DINFO, Florence, Italy*

Abstract

This overview paper describes the particle methods developed for the implementation of a class of Bayes filters formulated using the random finite set formalism. It is primarily intended for the readership already familiar with the particle methods in the context of the standard Bayes filter. The focus is on the Bernoulli particle filter, the probability hypothesis density (PHD) particle filter and the generalised labelled multi-Bernoulli (GLMB) particle filter. The performance of the described filters is demonstrated in the context of bearings-only target tracking application.

Keywords: Stochastic nonlinear filtering, Monte Carlo estimation, particle methods, random set models, target tracking, bearings-only measurements

*Corresponding author: B. Ristic, RMIT University, School of Electrical and Computer Engineering, Rm 10.8.14, 376-392 Swanston street, Melbourne, VIC 3000, Australia; email: branko.ristic@rmit.edu.au; tel: +61 3 9925 3768

Contents

1	Introduction	3
2	Particle methods for the standard Bayes filter	4
2.1	Problem formulation and the standard Bayes filter	5
2.2	A primer on the particle method	6
2.3	Calibration of system parameters	8
2.4	Demonstration: Bearings-only filtering	9
3	Background: FISST	10
3.1	Random finite sets	11
3.2	Some common RFS variables	14
4	Particle methods for the RFS Bayes-optimal filter	15
4.1	Formulation of the RFS Bayes-optimal filter	15
4.2	Particle method approximations	17
4.3	Bernoulli particle filter	20
4.4	Demonstration: Bearings-only detection and tracking	21
5	PHD particle filters	22
5.1	Formulation of the PHD filter	23
5.2	The particle method applied to PHD filtering	24
5.3	Calibration of tracking algorithms	29
5.4	Demonstration: Bearings-only multi-object filtering	30
6	Labelled RFS Bayes tracking filters	31
6.1	Labelled RFS	32
6.2	Labelled multi-object transition and likelihood models	34
6.3	δ -GLMB particle filter	35
6.4	Demonstration: Bearings-only multi-object tracking	42
7	Summary and further reading	43

Notation

\mathcal{X}	the single object state space
$\mathcal{F}(\mathcal{X})$	the multiple object state space
\mathcal{L}	the space of labels
\mathbf{x}	the state of a single object (a random vector)
\mathbf{X}	the state of multiple-objects (a random finite set, RFS)
\mathbb{X}	the state of multiple labelled objects (a labelled RFS)
\mathcal{Z}	measurement space
\mathbf{z}	a measurement of a single object (a random vector)
\mathbf{Z}	a detector output measurement (a RFS)
k	discrete-time index
$p(\mathbf{x})$	a probability density function (PDF) of $\mathbf{x} \in \mathcal{X}$
$\tilde{p}(\mathbf{x}, \ell)$	a PDF of a labelled random vector $(\mathbf{x}, \ell) \in \mathcal{X} \times \mathcal{L}$
$f(\mathbf{X})$	a PDF of an RFS variable $\mathbf{X} \in \mathcal{F}(\mathcal{X})$
$\tilde{f}(\mathbb{X})$	a PDF of a labelled RFS variable $\mathbb{X} \in (\mathcal{F}(\mathcal{X}) \times \mathcal{L})$

1. Introduction

In many areas of science and engineering there is a need to infer the behaviour of a stochastic dynamic system, using its partial and indirect observations. By combining (typically nonlinear) mathematical models of system evolution and sensor measurements, one can formulate the optimal sequential estimator in the Bayesian framework. This estimator, commonly referred to as the Bayes-optimal (or simply Bayes) filter, provides a recursive formula for the complete probabilistic characterisation of the dynamic system in the form of a time-varying posterior probability density of its state [1].

For most nonlinear/non-Gaussian formulations, analytic closed-form solutions of the Bayes filter are intractable. Practical solutions, therefore, need to be based on approximations. Particle filters are a class of Monte Carlo simulation based methods which can provide very accurate approximations of the Bayes filter. Despite being computationally expensive, particle filters have become universally popular, primarily due to their accuracy, relatively simple implementation and the ever increasing speed of computers. As a result of their widespread application, a few good tutorials and books have been published on the subject of particle filters [2], [3], [4], [5], [6], [7].

Particle filters have been introduced and traditionally applied as the approximate solutions of the *standard* Bayes filter, formulated during the 1960s [1] under the following assumptions: (i) the stochastic dynamic system (object,

phenomenon) is permanently active (or present); (ii) observations are noisy, but collected with perfect detection (i.e. there are no false or missed detections). All the aforementioned tutorials and books discuss the particle filters in this context only. However, in many practical applications, one may have to deal with multiple stochastic dynamic systems (objects), which can be simultaneously active (present), and which can randomly switch *on* and *off* (appear/disappear). In addition, perfect detection using surveillance sensors (e.g. radar, sonar, video cameras) is rarely possible [8]. Until recently, particle filters have been applied to this class of problems using a clever combination of Bayesian estimation theory with ad-hoc logic. However, the recent advances in Bayesian estimation using *random finite set* (RFS) models [9] resulted in elegant and rigorous mathematical formulations of the Bayes-optimal and principled Bayes-suboptimal filters, applicable to multiple interacting on/off switching systems with possibly imperfect detection of measurements.

This overview paper describes the particle methods developed for the implementation of the new class of RFS-Bayes filters. It is primarily intended for the readership already familiar with the particle methods in the context of the standard Bayes filter. One of the most popular and convincing applications of particle filters, versus standard approximation methods, such as the Extended Kalman filter (EKF) [10] and unscented Kalman filter (UKF) [11], has been for bearings-only tracking problems [5, Ch.6]. Hence, this application has been chosen to demonstrate throughout the paper different RFS-Bayes particle filters and their performance. The paper is organised as follows. Sec. 2 reviews the particle method for the standard Bayes filter. The elements of mathematics for random finite set models are presented in Sec. 3. The particle method for the RFS Bayes-optimal filter and its special case, the Bernoulli filter, are discussed in Sec. 4. A multi-target particle filter, referred to as the PHD particle filter, is presented in Sec. 5. The labelled RFS Bayes tracking filters implemented using the particle method are discussed in Sec. 6. The summary and pointers to advanced research topics are given in Sec. 7.

2. Particle methods for the standard Bayes filter

In order to familiarise with the notation, let us start with a quick review of the standard Bayes filter and the corresponding particle methods. The problem is by no means simple and it is still an active and highly relevant research topic.

2.1. Problem formulation and the standard Bayes filter

Suppose the state vector $\mathbf{x}_k \in \mathcal{X}$ provides the complete specification of the state of a dynamic system (object, phenomenon) at time t_k . Here $\mathcal{X} \subseteq \mathcal{R}^{n_x}$ is the state space, while k is the discrete-time index corresponding to t_k . Let us adopt the discrete-time additive-noise formulation, specified by two equations:

$$\mathbf{x}_k = \mathbf{f}_{k-1}(\mathbf{x}_{k-1}) + \mathbf{v}_{k-1}, \quad (1)$$

$$\mathbf{z}_k = \mathbf{h}_k(\mathbf{x}_k) + \mathbf{w}_k, \quad (2)$$

referred to as the *dynamics equation* and the *measurement equation*, respectively. Function $\mathbf{f}_{k-1} : \mathcal{R}^{n_x} \rightarrow \mathcal{R}^{n_x}$ in (1) is a nonlinear transition function defining the temporal evolution of the state vector as a first-order Markov process. Random disturbances $\mathbf{v}_k \in \mathcal{R}^{n_x}$, also known as process noise, are assumed to be independent identically distributed (IID) according to the probability density function (PDF) $p_{\mathbf{v}}$. Function $\mathbf{h}_k : \mathcal{R}^{n_x} \rightarrow \mathcal{R}^{n_z}$ in (2) defines the relationship between the state \mathbf{x}_k and the measurement $\mathbf{z}_k \in \mathcal{Z}$, where $\mathcal{Z} \subseteq \mathcal{R}^{n_z}$ is the measurement space. Random disturbances $\mathbf{w}_k \in \mathcal{R}^{n_z}$, also known as measurement noise, are assumed independent of \mathbf{v}_k , and modelled as an IID process with the PDF $p_{\mathbf{w}}$. Typically $n_z < n_x$, giving rise to the term *partial observations* of the system.

In the formulation specified by (1)-(2), the functions \mathbf{f}_k and \mathbf{h}_k , the probability distributions $p_{\mathbf{v}}$ and $p_{\mathbf{w}}$, and the PDF of the state vector at initial time $k = 0$, (i.e. $p_0(\mathbf{x}_0)$), are all assumed known. Equations (1) and (2) effectively define two probability functions: the *transitional density* $\pi_{k|k-1}(\mathbf{x}_k|\mathbf{x}_{k-1}) = p_{\mathbf{v}}(\mathbf{x}_k - \mathbf{f}_{k-1}(\mathbf{x}_{k-1}))$ and the *likelihood function* $g_k(\mathbf{z}_k|\mathbf{x}_k) = p_{\mathbf{w}}(\mathbf{z}_k - \mathbf{h}_k(\mathbf{x}_k))$. The problem is to compute recursively the posterior PDF of the state, denoted as $p_{k|k}(\mathbf{x}_k|\mathbf{z}_{1:k})$ at discrete-time k , where the notation $\mathbf{z}_{1:k}$ stands for the sequence $\mathbf{z}_1, \mathbf{z}_2, \dots, \mathbf{z}_k$.

The solution is usually presented as a two step procedure. Let $p_{k-1|k-1}(\mathbf{x}_{k-1}|\mathbf{z}_{1:k-1})$ denote the posterior PDF at $k-1$. The first step *predicts* the density of the state to time k via the Chapman-Kolmogorov equation [1]:

$$p_{k|k-1}(\mathbf{x}_k|\mathbf{z}_{1:k-1}) = \int \pi_{k|k-1}(\mathbf{x}_k|\mathbf{x}') p(\mathbf{x}'|\mathbf{z}_{1:k-1}) d\mathbf{x}'. \quad (3)$$

The second step applies Bayes rule to *update* $p(\mathbf{x}_k|\mathbf{z}_{1:k-1})$ using measurement \mathbf{z}_k :

$$p_{k|k}(\mathbf{x}_k|\mathbf{z}_{1:k}) = \frac{g_k(\mathbf{z}_k|\mathbf{x}_k) p_{k|k-1}(\mathbf{x}_k|\mathbf{z}_{1:k-1})}{\int g_k(\mathbf{z}_k|\mathbf{x}) p_{k|k-1}(\mathbf{x}|\mathbf{z}_{1:k-1}) d\mathbf{x}}. \quad (4)$$

Knowing the posterior $p_{k|k}(\mathbf{x}_k|\mathbf{z}_{1:k})$, one can compute a point estimate of the state $\hat{\mathbf{x}}_k$ (e.g. as the mean or the mode of the posterior) and a confidence (or credible) interval.

The closed-form analytic solution to (3)-(4) can be found only in some special cases. One important case is when \mathbf{f}_k and \mathbf{h}_k are linear functions and PDFs $p_{\mathbf{v}}$, $p_{\mathbf{w}}$ and p_0 are Gaussian; the solution in this case is the Kalman filter. In general, however, stochastic filtering via (3)-(4) can be solved only numerically. Many algorithms have been proposed for this purpose, including analytic approximations (e.g. Extended Kalman filter and its variants), grid-based methods (where the posterior PDF is evaluated at a finite and fixed set of points), Gaussian sum filters (where the posterior PDF is approximated by a Gaussian mixture), unscented transforms [11] and particle filters [5], [12].

2.2. A primer on the particle method

Suppose the posterior density at discrete-time $k - 1$ is approximated by a set of random samples (particles) $\{w_{k-1}^{(i)}, \mathbf{x}_{k-1}^{(i)}\}_{1 \leq i \leq N}$, where $\mathbf{x}_{k-1}^{(i)}$ is the state of particle i and $w_{k-1}^{(i)}$ is its weight. The weights are normalized, that is $\sum_{i=1}^N w_{k-1}^{(i)} = 1$. This approximation of the posterior improves as $N \rightarrow \infty$. Given $\{w_{k-1}^{(i)}, \mathbf{x}_{k-1}^{(i)}\}_{1 \leq i \leq N}$ and using the measurement \mathbf{z}_k at time k , the key question is how to form the particle approximation of the posterior at k , i.e. $p_{k|k}(\mathbf{x}_k | \mathbf{z}_{1:k})$, denoted $\{w_k^{(i)}, \mathbf{x}_k^{(i)}\}_{1 \leq i \leq N}$.

The computation of the weights and particles at time k is based on the concept of importance sampling [13]. Let us introduce a proposal or importance density $q_k(\mathbf{x}_k | \mathbf{x}_{k-1}, \mathbf{z}_k)$, whose support contains the support of the posterior PDF at time k . Then the (preliminary) particles at time k are drawn from the importance density:

$$\tilde{\mathbf{x}}_k^{(i)} \sim q_k(\mathbf{x}_k | \mathbf{x}_{k-1}^{(i)}, \mathbf{z}_k), \quad (5)$$

whose weights are computed as follows:

$$\tilde{w}_k^{(i)} = w_{k-1}^{(i)} \frac{g_k(\mathbf{z}_k | \tilde{\mathbf{x}}_k^{(i)}) \pi_{k|k-1}(\tilde{\mathbf{x}}_k^{(i)} | \mathbf{x}_{k-1}^{(i)})}{q_k(\tilde{\mathbf{x}}_k^{(i)} | \mathbf{x}_{k-1}^{(i)}, \mathbf{z}_k)} \quad (6)$$

$$w_k^{(i)} = \frac{\tilde{w}_k^{(i)}}{\sum_{j=1}^N \tilde{w}_k^{(j)}} \quad (7)$$

for $i = 1, \dots, N$. This recursive procedure starts at time $k = 0$ by sampling N times from the initial PDF p_0 .

The described particle method, also known as sequential importance sampling (SIS), inevitably fails after many iterations, because all particle weights, except a few, become zero (a poor approximation of the posterior PDF due to particle degeneracy). The collapse of the SIS scheme can be prevented by resampling the particles. The resampling step chooses N particles from

$\{w_k^{(i)}, \tilde{\mathbf{x}}_k^{(i)}\}_{1 \leq i \leq N}$, where the selection of particles is based on their weights: the probability of particle i being selected during resampling equals $w_k^{(i)}$. After resampling, all particle weights are equal to $1/N$. While resampling avoids degeneracy of particles, it leads to the loss of diversity among the particles, because the particles with large weights are selected (repeated) many times. In order to increase the particle diversity, it is usually recommended to perform a Markov chain Monte Carlo (MCMC) move step after resampling [14], [5], [6].

The choice of the importance density q_k plays an important role in the implementation of the particle filter (PF). The simplest choice is to select q_k as the transitional density, i.e. $q_k \equiv \pi_{k|k-1}$. This PF, referred to as the bootstrap filter [15], can lead to poor performance because many of the particles could be sampled from the region of the state space which is not in the support of the posterior (and therefore wasted). A better strategy is to use the information contained in the latest measurement \mathbf{z}_k in the design of the importance density. Research into good importance densities have resulted in many versions of the particle filter, such as: the optimal importance density (OID) PF [16], the auxiliary PF [17], the local-linearisation PF [16], [18], exact particle flow nonlinear filters [19], particle filters with progressive correction or tempering [20] and particle filters using Laplace approximation [21].

The bootstrap filter, being the simplest and possibly the most popular PF, is described in more detail and its pseudo code (for a single processing cycle at time k) is given in Alg. 1. Note that, since resampling is performed at the end of every cycle, there is no need to input/output particle weights. Recall also that after resampling it is recommended to carry out an MCMC move step.

Algorithm 1 Pseudo-code of the bootstrap filter

```

1: function BOOTSTRAP FILTER
2:   Input:  $\{\mathbf{x}_{k-1}^{(i)}\}_{1 \leq i \leq N}; \mathbf{z}_k$ 
3:   for  $i = 1, \dots, N$  do
4:     Draw a sample:  $\tilde{\mathbf{x}}_k^{(i)} \sim \pi_{k|k-1}(\mathbf{x}_k | \mathbf{x}_{k-1}^{(i)})$ 
5:     Calculate weight  $\tilde{w}_k^{(i)} = g_k(\mathbf{z}_k | \tilde{\mathbf{x}}_k^{(i)})$ 
6:   end for
7:    $w_k^{(i)} = \tilde{w}_k^{(i)} / \sum_{j=1}^N \tilde{w}_k^{(j)}$ , for  $i = 1, \dots, N$ 
8:   for  $i = 1, \dots, N$  do ▷ (Resampling)
9:     Select index  $j^i \in \{1, \dots, N\}$  with probability  $w_k^{(i)}$ 
10:     $\mathbf{x}_k^{(i)} = \tilde{\mathbf{x}}_k^{(j^i)}$ 
11:   end for
12:   Apply MCMC move and output  $\{\mathbf{x}_k^{(i)}\}_{1 \leq i \leq N}$ 
13: end function

```

A point estimate of the state at time k , denoted $\hat{\mathbf{x}}_k$, can be computed from

the particle approximation $\{w_k^{(i)}, \mathbf{x}_k^{(i)}\}_{1 \leq i \leq N}$ of the true posterior $p_k(\mathbf{x}_k | \mathbf{z}_{1:k})$ either: (a) as the weighted mean of the particles, referred to as the expected a posteriori (EAP) estimate, or (b) as the mode of the density estimated from the particles (using for example the kernel density estimation method, see [22]), referred to as the maximum a posteriori (MAP) estimate.

2.3. Calibration of system parameters

In many practical applications of nonlinear stochastic filtering, the transitional density and/or the likelihood function are dependent on a static parameter vector $\boldsymbol{\theta} \in \Theta \subseteq \mathcal{R}^{n_\theta}$. This is indicated in notation as $\pi_{k|k-1}(\mathbf{x}_k | \mathbf{x}_{k-1}, \boldsymbol{\theta})$ and $g_k(\mathbf{z}_k | \mathbf{x}_k, \boldsymbol{\theta})$. The problem is to estimate the posterior density $p(\boldsymbol{\theta} | \mathbf{z}_{1:k})$ (i.e. to calibrate the system) given its prior $p(\boldsymbol{\theta})$ and observations $\mathbf{z}_{1:k}$.

Note that according to Bayes rule $p(\boldsymbol{\theta} | \mathbf{z}_{1:k}) \propto \varrho(\mathbf{z}_{1:k} | \boldsymbol{\theta}) p(\boldsymbol{\theta})$, where $\varrho(\mathbf{z}_{1:k} | \boldsymbol{\theta})$ is the likelihood function. If we knew $\varrho(\mathbf{z}_{1:k} | \boldsymbol{\theta})$, we could apply standard Bayesian parameter estimation techniques (e.g. MCMC, population Monte Carlo [13]). In general, however, $\varrho(\mathbf{z}_{1:k} | \boldsymbol{\theta})$ cannot be expressed in closed-form. One natural option is to augment the state vector and carry out sequential Bayesian estimation on the joint space $\mathcal{X} \times \Theta$. Unfortunately, this is not a good idea, because the direct use of particle filtering in this case is inefficient [6] due to the absence of stochastic evolution for $\boldsymbol{\theta}$ (i.e. the particles in Θ space are sampled effectively only once).

The key idea of particle MCMC methods is to estimate the likelihood $\varrho(\mathbf{z}_{1:k} | \boldsymbol{\theta})$ using the particle filter [23]. Note first the following decomposition of the likelihood:

$$\varrho(\mathbf{z}_{1:k} | \boldsymbol{\theta}) = \varrho(\mathbf{z}_1 | \boldsymbol{\theta}) \prod_{t=2}^k \varrho(\mathbf{z}_t | \mathbf{z}_{1:t-1}, \boldsymbol{\theta}) \quad (8)$$

where the terms $\varrho(\mathbf{z}_t | \mathbf{z}_{1:t-1}, \boldsymbol{\theta})$ can be estimated from the un-normalised weights of the particles, see (6), at time step t [6]:

$$\varrho(\mathbf{z}_t | \mathbf{z}_{1:t-1}, \boldsymbol{\theta}) = \int g_t(\mathbf{z}_t | \mathbf{x}) p_{t|t-1}(\mathbf{x} | \mathbf{z}_{1:t-1}) d\mathbf{x} \approx \sum_{1 \leq i \leq N} \tilde{w}_t^{(i, \boldsymbol{\theta})}. \quad (9)$$

Using for example the Metropolis-Hasting MCMC algorithm, the parameter vector values $\boldsymbol{\theta}^*$ are iteratively generated from the proposal distribution $q(\boldsymbol{\theta} | \boldsymbol{\theta}')$ in order to be accepted or rejected. Note that for each proposed $\boldsymbol{\theta}^*$, one has to run the PF to estimate its likelihood $\varrho(\mathbf{z}_{1:k} | \boldsymbol{\theta}^*)$.

Suppose next that the parameter vector is also time varying. For example, its evolution may also be modeled by a first-order Markov process. In this case, although the inference needs to be made on the joint space $\mathcal{X} \times \Theta$, the particle

filter can be executed on sub-spaces Θ and $\mathcal{X}|\Theta$ because the posterior PDF can be factorized as $p_{k|k}(\mathbf{x}_k, \boldsymbol{\theta}_k | \mathbf{z}_{1:k}) = p_{k|k}(\mathbf{x}_k | \boldsymbol{\theta}_k, \mathbf{z}_{1:k}) p_{k|k}(\boldsymbol{\theta}_k | \mathbf{z}_{1:k})$. In some applications, the conditional posterior $p_{k|k}(\mathbf{x}_k | \boldsymbol{\theta}_k, \mathbf{z}_{1:k})$ is analytically tractable (e.g. linear/Gaussian case), which leads to the Rao-Blackwellised formulation of the marginalised PF [6], [24].

2.4. Demonstration: Bearings-only filtering

The problem of bearings-only filtering (or tracking) arises in a variety of important applications, including submarine tracking, using a passive sonar, and aircraft surveillance, using a radar in a passive mode [5]. The objective is to sequentially estimate the kinematics of a moving object using noise-corrupted bearing measurements. Two features of the problem are noteworthy [5],[25]: (a) the observation platform needs to manoeuvre in order to estimate the target range; (b) the problem becomes particularly difficult during the time steps when the bearings-rate is high. The particle filter, as a universal method for nonlinear filtering, has been demonstrated to outperform both EKF and UKF in this application¹ [5],[25].

Let us adopt the state vector of the moving object as

$$\mathbf{x}_k^m = \begin{bmatrix} x_k^m & y_k^m & \dot{x}_k^m & \dot{y}_k^m \end{bmatrix}^\top \quad (10)$$

where (x_k^m, y_k^m) and $(\dot{x}_k^m, \dot{y}_k^m)$ are its position and velocity in Cartesian coordinates, respectively. The observer state vector \mathbf{x}_k^o , which is known, is similarly defined. The dynamic (motion) model is written for the relative state vector, and is given by:

$$\mathbf{x}_k := \mathbf{x}_k^m - \mathbf{x}_k^o = \begin{bmatrix} x_k & y_k & \dot{x}_k & \dot{y}_k \end{bmatrix}^\top. \quad (11)$$

We adopt a nearly constant velocity (CV) motion model, as a linear version of (1):

$$\mathbf{x}_{k+1} = \mathbf{F}\mathbf{x}_k - \mathbf{U}_{k+1,k} + \mathbf{\Gamma}\mathbf{v}_k \quad (12)$$

where

$$\mathbf{F} = \begin{bmatrix} 1 & T \\ 0 & 1 \end{bmatrix} \otimes \mathbf{I}_2, \quad \mathbf{U}_{k+1,k} = \begin{bmatrix} x_{k+1}^o - x_k^o - T\dot{x}_k^o \\ y_{k+1}^o - y_k^o - T\dot{y}_k^o \\ \dot{x}_{k+1}^o - \dot{x}_k^o \\ \dot{y}_{k+1}^o - \dot{y}_k^o \end{bmatrix}, \quad \mathbf{\Gamma} = \begin{bmatrix} T^2/2 \\ T \end{bmatrix} \otimes \mathbf{I}_2. \quad (13)$$

¹Notice that the shifted Rayleigh filter [25], which is also a very accurate bearings-only filter, is not a universal nonlinear filter.

Explanation: \otimes is the Kroneker product; \mathbf{I}_n is identity matrix of dimension n ; $T = t_{k+1} - t_k$ is the (constant) sampling interval; \mathbf{F} is the transition matrix; $\mathbf{U}_{k+1,k}$ is a known deterministic matrix taking into account the effect of observer accelerations; $\mathbf{v}_k \sim \mathcal{N}(\mathbf{0}, \mathbf{Q})$ is white Gaussian process noise with $\mathbf{Q} = \sigma_v^2 \mathbf{I}_2$.

The available measurement at time k is the bearing measurement from the observer platform to the target, referenced clockwise positive to the y -axis and specified by a scalar version of (2):

$$z_k = h(\mathbf{x}_k) + w_k, \quad (14)$$

where $h(\mathbf{x}_k) = \text{atan2}(x_k, y_k)$ is the four-quadrant inverse tangent function and w_k is zero-mean white Gaussian noise with variance σ_w^2 .

Fig. 1 illustrates the scenario and the performance of the particle filter. Fig. 1.(a) shows the top-down observer-target geometry, together with the EAP estimates from the PF. This scenario was copied from [26], but considers only one of the targets (the full scenario with four targets that appear/disappear at different times, will be used later). The circles indicate the starting points of the two trajectories. Red dots indicate the cloud of particles at $t = 1200[\text{s}]$, $t = 1800[\text{s}]$ and $t = 2400[\text{s}]$. Figs. 1.(b) and (c) display the positional and velocity RMS error (over time), obtained by averaging over 100 Monte Carlo runs. The parameters used in simulations were as follows: $\sigma_w = 0.3^\circ$, $T = 20[\text{s}]$, $\sigma_v = 0.005 [\text{m/s}^2]$, $N = 5000$ particles. Nonlinear filtering was carried out during the period when the target was present, that is from $t = 200[\text{s}]$ to $t = 2400[\text{s}]$, which corresponds to 111 discrete-time steps. Note that Fig. 1.(a) also shows the clouds of particles at time instances 1200[s], 1800[s] and 2400[s].

The particle filter is initialised by drawing samples from the *initial* or *birth* density designed using the first bearing measurement z_1 , as well as prior knowledge of (i) the sensor range r_{\max} and (ii) the maximum speed of the target v_{\max} . The birth density in target position is the sector of a circle (“pizza slice”), centred at the observer position at $k = 1$, i.e. (x_1^o, y_1^o) , determined by the angles $z_1 \pm 3\sigma_w$ and the radius $r_{\max} = 10000[\text{m}]$. The target birth density in velocity is uniform PDF $\mathcal{U}[-v_{\max}, +v_{\max}]$ in both \dot{x}_1^m and \dot{y}_1^m , with $v_{\max} = 7.5 [\text{m/s}]$.

3. Background: FISST

The prerequisite for the random finite set formulation of the Bayes-optimal filter is advanced mathematics, referred to as *finite set statistics* (FISST) [27], developed by Ron Mahler. This section will introduce only the bare minimum necessary to follow the rest of the paper. The full theoretical details are beyond

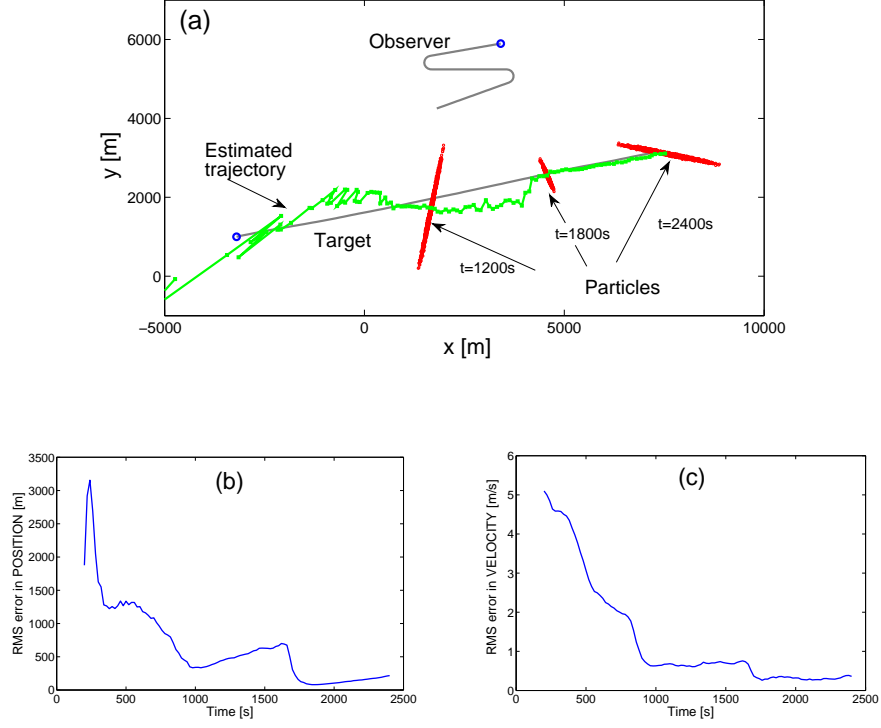


Figure 1: Particle filter applied to bearings-only filtering problem ($\sigma_w = 0.3^\circ$): (a) top-down view of the scenario and the estimated trajectory (red dots are particle clouds); (b) RMS error in position; (c) RMS error in velocity

the scope of this paper, however the proofs and derivations can be found in Mahler's excellent books [27, Part II] and [9, Part I].

3.1. Random finite sets

A random finite set is a convenient probabilistic model for the representation of multiple stochastic dynamic systems (objects) and sensor measurements. Suppose that at discrete-time k there are n_k objects with states $\mathbf{x}_{k,1}, \dots, \mathbf{x}_{k,n_k}$, taking values in the state space $\mathcal{X} \subseteq \mathcal{R}^{n_x}$. Both the number of dynamic objects n_k and their individual states in \mathcal{X} are random and time-varying. The multi-object state at k is a finite set

$$\mathbf{X}_k = \{\mathbf{x}_{k,1}, \dots, \mathbf{x}_{k,n_k}\} \in \mathcal{F}(\mathcal{X}), \quad (15)$$

which can be modelled as a random finite set on \mathcal{X} . Here $\mathcal{F}(\mathcal{X})$ is the set of finite subsets of \mathcal{X} .

Typically, the detection process is imperfect, meaning that not all of the objects in \mathbf{X}_k are detected, while spurious (false) detections may be created due to background noise and interferences. Suppose that \mathbf{Z}_k is a measurement set from such a detector, reported at time k . Then

$$\mathbf{Z}_k = \{\mathbf{z}_{k,1}, \dots, \mathbf{z}_{k,m_k}\} \in \mathcal{F}(\mathcal{Z}), \quad (16)$$

can also be modelled by a random finite set on the observation space $\mathcal{Z} \subseteq \mathcal{R}^{n_z}$. Both the cardinality $m_k = |\mathbf{Z}_k|$ and the individual states in \mathcal{Z} are random. Here $\mathcal{F}(\mathcal{Z})$ is the set of finite subsets of \mathcal{Z} .

A random finite set (RFS) variable is a random variable that takes values as unordered finite sets. The cardinality of an RFS variable \mathbf{X} is random and modelled by a discrete distribution $\rho(n) = \Pr\{|\mathbf{X}| = n\}$, where n is a non-negative integer, $n \in \mathbb{N} \cup \{0\}$. An RFS \mathbf{X} is completely specified by its cardinality distribution $\rho(n)$ and a family of symmetric joint distributions² $p_n(\mathbf{x}_1, \dots, \mathbf{x}_n)$, that characterise the distribution of its elements over the state space, conditioned on cardinality n .

Since an RFS is nothing but a finite-set valued random variable, the usual probabilistic descriptors of a random variable, such as the PDF and its statistical moments, can be defined for it. FISST provides the tools for mathematical representation and manipulation of random finite sets³. The FISST PDF of an RFS variable \mathbf{X} is denoted $f(\mathbf{X})$ and defined as:

$$f(\{\mathbf{x}_1, \dots, \mathbf{x}_n\}) = n! \cdot \rho(n) \cdot p_n(\mathbf{x}_1, \dots, \mathbf{x}_n). \quad (17)$$

For example, $f(\emptyset) = \rho(0)$, $f(\{\mathbf{x}\}) = \rho(1)p(\mathbf{x})$, $f(\{\mathbf{x}_1, \mathbf{x}_2\}) = 2\rho(2)p_2(\mathbf{x}_1, \mathbf{x}_2)$, etc. Note that $f(\emptyset)$, $f(\{\mathbf{x}\})$, $f(\{\mathbf{x}_1, \mathbf{x}_2\})$, etc, have different units. Throughout the text, we will refer to the FISST densities as to the multi-object PDFs.

Being a PDF, $f(\mathbf{X})$ should integrate to one. However, the standard integral cannot be applied; instead we need to introduce the *set integral*, defined as

²A joint distribution function $p_n(\mathbf{x}_1, \dots, \mathbf{x}_n)$ is said to be symmetric if its value remains unchanged for all of the $n!$ possible permutations of its variables.

³Note that while the FISST densities are not probability densities, they have been shown to be equivalent to probability densities on $\mathcal{F}(X)$ relative to some reference measure [28]. Subsequently, we do not distinguish between FISST densities and probability densities of random finite sets.

follows:

$$\int f(\mathbf{X}) \delta \mathbf{X} := f(\emptyset) + \sum_{n=1}^{\infty} \frac{1}{n!} \int f(\{\mathbf{x}_1, \dots, \mathbf{x}_n\}) d\mathbf{x}_1 \cdots d\mathbf{x}_n \quad (18)$$

Now it is straightforward to verify that indeed $f(\mathbf{X})$ integrates to 1:

$$\begin{aligned} \int f(\mathbf{X}) \delta \mathbf{X} &= \rho(0) + \sum_{n=1}^{\infty} \rho(n) \underbrace{\int p_n(\mathbf{x}_1, \dots, \mathbf{x}_n) d\mathbf{x}_1 \cdots d\mathbf{x}_n}_{=1, \text{ being a standard PDF}} \\ &= \sum_{n=0}^{\infty} \rho(n) = 1 \quad (\text{since } \rho(n) \text{ is a discrete distribution}) \end{aligned}$$

The cardinality distribution $\rho(n)$ of an RFS variable \mathbf{X} can be obtained from the multi-object PDF $f(\mathbf{X})$ as:

$$\rho(n) = \frac{1}{n!} \int f(\{\mathbf{x}_1, \dots, \mathbf{x}_n\}) d\mathbf{x}_1 \cdots d\mathbf{x}_n \quad (19)$$

The *intensity function* (also known as the probability hypothesis density or PHD) is an important characterisation of an RFS \mathbf{X} on \mathcal{X} , defined as its first-order statistical moment. In order to define the PHD function, let us first introduce the set Dirac delta function

$$\delta_{\mathbf{X}}(\mathbf{x}) = \sum_{\mathbf{w} \in \mathbf{X}} \delta_{\mathbf{w}}(\mathbf{x})$$

with $\delta_{\mathbf{w}}(\mathbf{x})$ being the standard Dirac delta function concentrated at \mathbf{w} . Now we can express the cardinality of an RFS \mathbf{X} as follows:

$$|\mathbf{X}| = \int_{\mathcal{X}} \delta_{\mathbf{X}}(\mathbf{x}) d\mathbf{x}. \quad (20)$$

We would like to define the PHD function $D(\mathbf{x})$ of \mathbf{X} in such a way that the expected cardinality of \mathbf{X} over the state space \mathcal{X} is obtained as the integral

$$\mathcal{E}\{|\mathbf{X}|\} = \int_{\mathcal{X}} D(\mathbf{x}) d\mathbf{x}. \quad (21)$$

Since

$$\mathcal{E}\{|\mathbf{X}|\} \triangleq \int |\mathbf{X}| f(\mathbf{X}) \delta \mathbf{X} \quad (22)$$

$$= \int \left[\int_{\mathcal{X}} \delta_{\mathbf{X}}(\mathbf{x}) d\mathbf{x} \right] f(\mathbf{X}) \delta \mathbf{X} \quad (23)$$

$$= \int_{\mathcal{X}} \left[\int \delta_{\mathbf{X}}(\mathbf{x}) f(\mathbf{X}) \delta \mathbf{X} \right] d\mathbf{x}, \quad (24)$$

comparing (21) with (24), notice that

$$D(\mathbf{x}) \triangleq \mathcal{E}\{\delta_{\mathbf{X}}(\mathbf{x})\} = \int \delta_{\mathbf{X}}(\mathbf{x}) f(\mathbf{X}) \delta \mathbf{X}. \quad (25)$$

Here $\mathcal{E}\{\delta_{\mathbf{X}}(\mathbf{x})\}$ is the expected value (the first statistical moment) of the RFS \mathbf{X} . Note that $D(\mathbf{x})$ is a density function on the state space \mathcal{X} .

In general, the PHD function $D(\mathbf{x})$ and the cardinality distribution $\rho(n)$ do not completely characterize the multi-object PDF. However, we will see in the next section that for some specific RFSs, the characterization is complete.

3.2. Some common RFS variables

Bernoulli RFS. This RFS can either be empty (with probability $1 - r$) or have one element (with probability r), spatially distributed over \mathcal{X} according to the (standard) PDF $p(\mathbf{x})$. The FISST PDF of the Bernoulli RFS \mathbf{X} is given by:

$$f(\mathbf{X}) = \begin{cases} 1 - r, & \text{if } \mathbf{X} = \emptyset \\ r \cdot p(\mathbf{x}), & \text{if } \mathbf{X} = \{\mathbf{x}\}. \end{cases} \quad (26)$$

The intensity function of the Bernoulli RFS \mathbf{X} is $D(\mathbf{x}) = r \cdot p(\mathbf{x})$.

IID Cluster RFS. Let the cardinality distribution of independent identically distributed (IID) cluster RFS \mathbf{X} be $\rho(n)$. For a given cardinality, the elements of \mathbf{X} are each IID random variables distributed according to the (standard) PDF $p(\mathbf{x})$ on \mathcal{X} . The multi-object PDF of \mathbf{X} is:

$$f(\mathbf{X}) = |\mathbf{X}|! \cdot \rho(|\mathbf{X}|) \prod_{\mathbf{x} \in \mathbf{X}} p(\mathbf{x}) \quad (27)$$

The main simplification in comparison with (17) is that due to the IID property, the symmetric joint distribution is replaced by a product. The intensity function of an IID cluster RFS is:

$$D(\mathbf{x}) = p(\mathbf{x}) \sum_{n=1}^{\infty} n \rho(n) \quad (28)$$

Poisson RFS. If the cardinality distribution of an IID cluster RFS is Poisson with parameter $\lambda > 0$, i.e.

$$\rho(n) = \frac{e^{-\lambda} \lambda^n}{n!}, \quad n = 0, 1, 2, \dots \quad (29)$$

then this RFS is referred to as the Poisson RFS \mathbf{X} . Its multi-object PDF follows from (27) and is given by:

$$f(\mathbf{X}) = e^{-\lambda} \prod_{\mathbf{x} \in \mathbf{X}} \lambda p(\mathbf{x}) \quad (30)$$

while its intensity function is

$$D(\mathbf{x}) = \lambda p(\mathbf{x}). \quad (31)$$

The Poisson RFS is the only RFS which is completely specified by its intensity function, because knowledge of λ and $p(\mathbf{x})$ fully determines the multi-object PDF in (30). Both λ and $p(\mathbf{x})$ can be worked out from $D(\mathbf{x})$: λ is the expected cardinality of \mathbf{X} , i.e. $\mathcal{E}\{|\mathbf{X}|\} = \int D(\mathbf{x}) d\mathbf{x} = \lambda$, while $p(\mathbf{x}) = D(\mathbf{x})/\lambda$.

Multi-Bernoulli RFS. A multi-Bernoulli RFS \mathbf{X} is a union of independent Bernoulli RFSs \mathbf{X}_i , each characterized by existence probability r_i and the spatial PDF $p_i(\mathbf{x})$, for $i = 1, \dots, M$:

$$\mathbf{X} = \bigcup_{i=1}^M \mathbf{X}_i.$$

The multi-object PDF of $\mathbf{X} = \{\mathbf{x}_1, \dots, \mathbf{x}_n\}$ is given by:

$$f(\mathbf{X}) = n! \left[\prod_{j=1}^M (1 - r_j) \right] \cdot \sum_{1 \leq i_1 < \dots < i_n \leq M} \frac{r_{i_1} p_{i_1}(\mathbf{x}_1)}{1 - r_{i_1}} \dots \frac{r_{i_n} p_{i_n}(\mathbf{x}_n)}{1 - r_{i_n}}. \quad (32)$$

For example, $f(\emptyset) = \prod_{j=1}^M (1 - r_j)$, $f(\{\mathbf{x}\}) = f(\emptyset) \sum_{i=1}^M \frac{r_i p_i(\mathbf{x})}{1 - r_i}$, etc. Note that the pairs $(r_i, p_i(\mathbf{x}))$, $i = 1, \dots, M$, fully specify the multi-object PDF (32). Consequently, they also determine the intensity function of the multi-Bernoulli RFS, which is given by: $D(\mathbf{x}) = \sum_{i=1}^M r_i p_i(\mathbf{x})$.

4. Particle methods for the RFS Bayes-optimal filter

4.1. Formulation of the RFS Bayes-optimal filter

The goal of the RFS Bayes-optimal filter is to estimate the posterior density of a multi-object state, represented by the RFS variable \mathbf{X}_k . Evolution of \mathbf{X}_k is modelled by a Markov process, characterized by its initial FISST density $f_0(\mathbf{X}_0)$ and the FISST transitional density $\Pi_{k|k-1}(\mathbf{X}_k|\mathbf{X}_{k-1})$. The standard case of $\Pi_{k|k-1}(\mathbf{X}_k|\mathbf{X}_{k-1})$ has been derived in Chapter 13 of [27] as the union of a multi-Bernoulli object survival RFS and a Poisson birth RFS, under the assumption that the constituent RFSs are mutually independent. It can be expressed in a compact form as:

$$\Pi_{k|k-1}(\mathbf{X}|\mathbf{X}') = f_b(\mathbf{X})(1 - p_s)^{|\mathbf{X}'|} \sum_{\theta} \prod_{i:\theta(i)>0} \frac{p_s \cdot \pi_{k|k-1}(\mathbf{x}_{\theta(i)}|\mathbf{x}'_i)}{(1 - p_s) \cdot \mu_0 b_k(\mathbf{x}_{\theta(i)})} \quad (33)$$

where $\theta : \{1, \dots, |\mathbf{X}'|\} \rightarrow \{0, 1, \dots, |\mathbf{X}|\}$ represents a list of all possible assignments of elements from the set \mathbf{X}' to the elements of the set \mathbf{X} (here the

assumptions are that $|\mathbf{X}'| > 0$ and $|\mathbf{X}| \geq 0$); p_s is the probability of object survival from time $k-1$ to k ; $f_b(\mathbf{X})$ is the object birth multi-object PDF, which assuming a Poisson birth process with the mean rate μ_0 and distribution $b_k(\mathbf{x})$, according to (30) is given by:

$$f_b(\mathbf{X}) = e^{-\mu_0} \prod_{\mathbf{x} \in \mathbf{X}} \mu_0 b_k(\mathbf{x}).$$

Finally, $\pi_{k|k-1}(\mathbf{x}|\mathbf{x}')$ is the (standard) transitional density, defined in Sec. 2.1.

The multi-object state \mathbf{X}_k is not observed directly, but through the observation process, assumed to be conditionally independent given the multi-object state process, and fully specified by the (multi-object) likelihood function. Many different observation models have been considered in the literature, such as the models for intensity measurements versus detector-output measurements⁴, extended versus point target measurements, finite resolution measurements, fuzzy or imprecise measurements, see for details [29], [30], [72], [9], [26].

The detector-output measurement model for a point-size target, referred to as the standard model [27],[9], will be adopted throughout this tutorial. Recall from (16) that the standard measurement is modelled by an RFS variable \mathbf{Z}_k . The likelihood function $\varphi_k(\mathbf{Z}_k|\mathbf{X}_k)$ for this model has been derived in Chapter 12 of [27] as the superposition of a multi-Bernoulli object-detection RFS and a Poisson clutter (false detection) RFS. Under the assumption that the constituent RFSs are mutually independent, the multi-object likelihood function can be expressed by:

$$\varphi_k(\mathbf{Z}|\mathbf{X}) = f_c(\mathbf{Z})(1 - p_D)^{|\mathbf{X}|} \sum_{\theta} \prod_{i:\theta(i)>0} \frac{p_D \cdot g_k(\mathbf{z}_{\theta(i)}|\mathbf{x}_i)}{(1 - p_D) \cdot \lambda c(\mathbf{z}_{\theta(i)})}. \quad (34)$$

Explanation: $\theta : \{1, \dots, |\mathbf{X}|\} \rightarrow \{0, 1, \dots, |\mathbf{Z}|\}$ represents a list of all associations of elements from set \mathbf{X} to the elements of set \mathbf{Z} (here the assumption is that if $\mathbf{x}_i \in \mathbf{X}$ is not detected, then $\theta(i) = 0$; also, a target $\mathbf{x} \in \mathbf{X}$ can generate at most one measurement $\mathbf{z} \in \mathbf{Z}$); p_D is the probability of detection; $f_c(\mathbf{Z})$ is the multi-object PDF of clutter, which is assumed to be a Poisson RFS with the mean rate λ and distribution $c(\mathbf{z})$ over \mathcal{Z} . According to (30), the clutter

⁴An intensity measurement at time k represents a raw sensor measurement, prior to detection thresholding. In tracking literature this is also referred to as track-before-detect approach. Using intensity measurements (rather than the detector-output measurements) can lead to the better error performance, but at increased computational load due to the large data flow. An intensity measurement at time k is a vector, rather than a random finite set. A detailed explanation with examples of intensity measurement models can be found in [29].

multi-object PDF is:

$$f_c(\mathbf{Z}) = e^{-\lambda} \prod_{\mathbf{z} \in \mathbf{Z}} \lambda c(\mathbf{z}). \quad (35)$$

Finally, $g_k(\mathbf{z}|\mathbf{x})$ in (34) is the conventional likelihood function, introduced in Sec. 2.1.

Given \mathbf{X}_k , measurement \mathbf{Z}_k is assumed to be statistically independent of \mathbf{Z}_ℓ , where $\ell \neq k$. The Bayes-optimal filtering problem can now be cast in the random finite set framework. Suppose that at time $k-1$ the posterior FISST PDF of the multi-object state, $f_{k-1|k-1}(\mathbf{X}_{k-1}|\mathbf{Z}_{1:k-1})$ is known. Here $\mathbf{Z}_{1:k-1} \equiv \mathbf{Z}_1, \dots, \mathbf{Z}_{k-1}$ is the sequence of all previous measurements. Then the predicted and updated posterior multi-object densities can be expressed as follows [27]:

$$f_{k|k-1}(\mathbf{X}_k|\mathbf{Z}_{1:k-1}) = \int \Pi_{k|k-1}(\mathbf{X}_k|\mathbf{X}') f_{k-1|k-1}(\mathbf{X}'|\mathbf{Z}_{1:k-1}) \delta \mathbf{X}' \quad (36)$$

$$f_{k|k}(\mathbf{X}_k|\mathbf{Z}_{1:k}) = \frac{\varphi_k(\mathbf{Z}_k|\mathbf{X}_k) f_{k|k-1}(\mathbf{X}_k|\mathbf{Z}_{1:k-1})}{\int \varphi_k(\mathbf{Z}_k|\mathbf{X}) f_{k|k-1}(\mathbf{X}|\mathbf{Z}_{1:k-1}) \delta \mathbf{X}}, \quad (37)$$

respectively.

The recursion (36)-(37) is a non-trivial generalisation of (3)-(4), because the integrals in (36)-(37) are set integrals and the expressions for $\Pi_{k|k-1}(\mathbf{X}_k|\mathbf{X}_{k-1})$ and $\varphi_k(\mathbf{Z}_k|\mathbf{X}_k)$ are quite involved. Computing the exact multi-object posterior density is numerically intractable and all practical algorithms are based on approximations. An important feature of the RFS Bayes-optimal filter is that it performs multi-object filtering, as opposed to target (object) tracking. The difference is significant: a point estimate from the multi-object filter, at each time step, is a collection of (unlabelled and unordered) object state estimates; a multi-target tracker, on the other hand, produces labelled state trajectory estimates, or tracks.

4.2. Particle method approximations

Implementation of the RFS Bayes-optimal filter using the particle method has been considered in the past, both assuming the intensity measurement model (typically without a reference to RFS models, e.g. [31]) and the standard measurement model [32], [33], [28], [34], [35], [36]. Since the filter is defined on the set of subsets $\mathcal{F}(\mathcal{X})$, it is computationally very demanding and practical only for a small number of objects. A particle in the state space $\mathcal{F}(\mathcal{X})$ can be expressed

as:

$$\mathbf{X}_k^{(i)} = \begin{cases} \emptyset, & \text{if } |\mathbf{X}_k^{(i)}| = 0 \\ [\mathbf{x}_k^{(i)}], & \text{if } |\mathbf{X}_k^{(i)}| = 1 \\ [(\mathbf{x}_{k,1}^{(i)})^\top (\mathbf{x}_{k,2}^{(i)})^\top]^\top, & \text{if } |\mathbf{X}_k^{(i)}| = 2 \\ \dots & \\ [(\mathbf{x}_{k,1}^{(i)})^\top (\mathbf{x}_{k,2}^{(i)})^\top \dots (\mathbf{x}_{k,\nu_{\max}}^{(i)})^\top]^\top, & \text{if } |\mathbf{X}_k^{(i)}| = \nu_{\max} \end{cases} \quad (38)$$

where ν_{\max} denotes the maximum number of targets (a design parameter). Note that particle $i = 1, 2, \dots, N$, for a given cardinality, is represented in (38) by a vector. While this was done to simplify computer implementation, one should keep in mind that the multi-object particle essentially represents a random finite set, that is, any permutation of its elements (objects, targets) results in the equivalent particle. By ignoring the permutation equivalence, the multi-object state particle filter can be affected by the *mixed labelling* problem, see [37]. It has been noted that mixed labeling is typically resolved after few time steps due to resampling step in the particle filter [37].

The pseudo-code of the bootstrap-type particle filter which implements a cycle of the RFS Bayes-optimal filter at time k is given in Alg. 2. The proposed multi-object particles at time k are constructed based on the transitional density, the survival probability and the birth distribution of new targets, ignoring the association events in (33). The average number of newborn targets is μ_0 , with birth distribution $b_k(\mathbf{x})$ in line 14 typically designed using the measurements from time $k - 1$. The computation of the multi-object likelihood $\varphi_k(\mathbf{Z}_k|\mathbf{X}_k^{(i)})$ in line 17, defined in (34), requires the evaluation all association hypotheses θ between objects in $\mathbf{X}_k^{(i)}$ and detections in \mathbf{Z}_k . The number of these hypotheses grows exponentially with the number of targets. For example, if the cardinalities are: $|\mathbf{X}_k^{(i)}| = 2$ and $|\mathbf{Z}_k| = 3$, the number of association hypothesis ⁵ is 13. This exponentially growing computational cost is the major limitation of the RFS Bayes-optimal filter in practice.

Estimation of the multi-object state \mathbf{X}_k from the particle approximation of the posterior $f_{k|k}(\mathbf{X}_k|\mathbf{Z}_{1:k})$ is discussed briefly next. The cardinality distribution

⁵In this case $\theta : \{\mathbf{x}_1, \mathbf{x}_2\} \rightarrow \{\emptyset, \mathbf{z}_1, \mathbf{z}_2, \mathbf{z}_3\}$, because targets can be undetected. The list of possible assignments is: $\theta_1 : \mathbf{x}_1 \rightarrow \emptyset; \mathbf{x}_2 \rightarrow \emptyset$; $\theta_2 : \mathbf{x}_1 \rightarrow \emptyset; \mathbf{x}_2 \rightarrow \mathbf{z}_1$; $\theta_3 : \mathbf{x}_1 \rightarrow \emptyset; \mathbf{x}_2 \rightarrow \mathbf{z}_2$; $\theta_4 : \mathbf{x}_1 \rightarrow \emptyset; \mathbf{x}_2 \rightarrow \mathbf{z}_3$; $\theta_5 : \mathbf{x}_1 \rightarrow \mathbf{z}_1; \mathbf{x}_2 \rightarrow \emptyset$; $\theta_6 : \mathbf{x}_1 \rightarrow \mathbf{z}_1; \mathbf{x}_2 \rightarrow \mathbf{z}_2$; $\theta_7 : \mathbf{x}_1 \rightarrow \mathbf{z}_1; \mathbf{x}_2 \rightarrow \mathbf{z}_3$; $\theta_8 : \mathbf{x}_1 \rightarrow \mathbf{z}_2; \mathbf{x}_2 \rightarrow \emptyset$; $\theta_9 : \mathbf{x}_1 \rightarrow \mathbf{z}_2; \mathbf{x}_2 \rightarrow \mathbf{z}_1$; $\theta_{10} : \mathbf{x}_1 \rightarrow \mathbf{z}_2; \mathbf{x}_2 \rightarrow \mathbf{z}_3$; $\theta_{11} : \mathbf{x}_1 \rightarrow \mathbf{z}_3; \mathbf{x}_2 \rightarrow \emptyset$; $\theta_{12} : \mathbf{x}_1 \rightarrow \mathbf{z}_3; \mathbf{x}_2 \rightarrow \mathbf{z}_1$; $\theta_{13} : \mathbf{x}_1 \rightarrow \mathbf{z}_3; \mathbf{x}_2 \rightarrow \mathbf{z}_2$.

Algorithm 2 Pseudo-code of the RFS bootstrap filter

```

1: function RFS BOOTSTRAP FILTER
2:   Input:  $\{\mathbf{X}_{k-1}^{(i)}\}_{1 \leq i \leq N}$ ,  $\mathbf{Z}_k$ 
3:   for  $i = 1, \dots, N$  do
4:      $\tilde{\mathbf{X}}_k^{(i)} = []$ 
5:     for  $j = 1, \dots, |\mathbf{X}_{k-1}^{(i)}|$  do
6:        $u_* \sim \mathcal{U}_{[0,1]}$ 
7:       if  $u_* < p_S$  then
8:          $\mathbf{x}_* \sim \pi_{k|k-1}(\mathbf{x}|\mathbf{X}_{k-1,j}^{(i)})$ 
9:          $\tilde{\mathbf{X}}_k^{(i)} = [(\tilde{\mathbf{X}}_k^{(i)})^\top \mathbf{x}_*^\top]^\top$ 
10:        end if
11:      end for
12:       $\mu \sim \text{Poisson}(\mu_0)$ 
13:      for  $j = 1, \dots, \mu$  do
14:         $\mathbf{x}_* \sim b_k(\mathbf{x})$ 
15:         $\tilde{\mathbf{X}}_k^{(i)} = [(\tilde{\mathbf{X}}_k^{(i)})^\top \mathbf{x}_*^\top]^\top$ 
16:      end for
17:      Calculate weight:  $\tilde{w}_k^{(i)} = \varphi_k(\mathbf{Z}_k|\tilde{\mathbf{X}}_k^{(i)})$ 
18:    end for
19:     $w_k^{(i)} = \tilde{w}_k^{(i)} / \sum_{j=1}^N \tilde{w}_k^{(j)}$ , for  $i = 1, \dots, N$ 
20:    for  $i = 1, \dots, N$  do
21:      Select index  $j^i \in \{1, \dots, N\}$  with probability  $w_k^{(i)}$ 
22:       $\mathbf{X}_k^{(i)} = \tilde{\mathbf{X}}_k^{(j^i)}$ 
23:    end for
24:    Output:  $\{\mathbf{X}_k^{(i)}\}_{1 \leq i \leq N}$ 
25: end function

```

can be estimated as:

$$\hat{\rho}_{k|k}(n|\mathbf{Z}_{1:k}) = \frac{1}{N} \sum_{i=1}^N \delta[|\mathbf{X}_k^{(i)}|, n], \quad n = 0, 1, 2, \dots, \nu_{\max}, \quad (39)$$

where $\delta[\ell, n]$ is the Kronecker delta function which equals 1 if $\ell = n$ and zero otherwise. Practically, for each $n = 0, 1, \dots, \nu_{\max}$, it is necessary to count the number of multi-target particles whose cardinality equals n , and then to divide this count with the total number of particles N . Then one can estimate the number of targets in \mathbf{X}_k , that is $\hat{n}_{k|k}$, either as the expected value or the maximum of the posterior $\hat{\rho}_{k|k}(n|\mathbf{Z}_{1:k})$. Given $\hat{n}_{k|k}$, the multi-target state can be estimated from the particle system $\{w_k^{(i)}, \mathbf{X}_k^{(i)}\}_{1 \leq i \leq N}$ as

$$\hat{\mathbf{X}}_k = \frac{\sum_{i=1}^N w_k^{(i)} \mathbf{X}_k^{(i)} \delta[|\mathbf{X}_k^{(i)}|, \hat{n}_k]}{\sum_{i=1}^N w_k^{(i)} \delta[|\mathbf{X}_k^{(i)}|, \hat{n}_k]}, \quad (40)$$

which represents the mean of the multi-target particles characterized by cardinality $\hat{n}_{k|k}$.

4.3. Bernoulli particle filter

The Bernoulli filter is the special case of the RFS Bayes-optimal filter, derived by Mahler [27] under the assumption that \mathbf{X}_k is a Bernoulli RFS. Recall that the Bernoulli RFS \mathbf{X} can have zero or one element and its PDF $f(\mathbf{X})$ is completely specified by: (1) the probability of object existence r and (2) the PDF $p(\mathbf{x})$ on \mathcal{X} . Hence, the Bernoulli filter is the Bayes-optimal filter for joint detection and tracking of a single object, where detection is carried out by monitoring the posterior probability of object existence.

A detailed tutorial on Bernoulli filters, their formulation for different measurement models, their numerical implementation and various applications can be found in [29]. Here we present only the prediction and update equations for the standard measurement model. Suppose the posterior $f_{k-1|k-1}(\mathbf{X}|\mathbf{Z}_{1:k-1})$ is known and specified by the pair $(r_{k-1|k-1}, p_{k-1|k-1}(\mathbf{x}))$. The prediction equations of the Bernoulli filter are given by:

$$r_{k|k-1} = p_b(1 - r_{k-1|k-1}) + p_s r_{k-1|k-1} \quad (41)$$

$$p_{k|k-1}(\mathbf{x}) = \frac{p_b(1 - r_{k-1|k-1})b_{k|k-1}(\mathbf{x})}{r_{k|k-1}} + \frac{p_s r_{k-1|k-1} \int \pi_{k|k-1}(\mathbf{x}|\mathbf{x}')p_{k-1|k-1}(\mathbf{x}')d\mathbf{x}'}{r_{k|k-1}} \quad (42)$$

where p_b is the probability of object “birth” from the previous time $k-1$ to k and $b_{k|k-1}(\mathbf{x})$ is the object birth density. The update equations are as follows:

$$r_{k|k} = \frac{1 - \Delta_k}{1 - r_{k|k-1}\Delta_k} r_{k|k-1} \quad (43)$$

$$p_{k|k}(\mathbf{x}) = \frac{1 - p_D + p_D \sum_{\mathbf{z} \in \mathbf{Z}_k} \frac{g_k(\mathbf{z}|\mathbf{x})}{\lambda c(\mathbf{z})}}{1 - \Delta_k} p_{k|k-1}(\mathbf{x}) \quad (44)$$

where, assuming p_D is independent of the state,

$$\Delta_k = p_D \left(1 - \sum_{\mathbf{z} \in \mathbf{Z}_k} \frac{\int g_k(\mathbf{z}|\mathbf{x})p_{k|k-1}(\mathbf{x})d\mathbf{x}}{\lambda c(\mathbf{z})} \right). \quad (45)$$

It can be verified that if $r_{k-1|k-1} = 1$, $p_b = 0$, $p_D = 1$ and $\lambda = 0$, the Bernoulli filter equations reduce to the standard Bayes filter equations (3)-(4).

The Bernoulli particle filter propagates through time the scalar value of $r_{k|k}$ and the weighted particle system $\{w_k^{(i)}, \mathbf{x}_k^{(i)}\}_{1 \leq i \leq N}$. The pseudo-code of the Bernoulli bootstrap-type particle filter is given in Alg. 3. It implements the birth density in (42) as $b_{k|k-1}(\mathbf{x}) = \int \pi_{k|k-1}(\mathbf{x}|\mathbf{x}')b_{k-1}(\mathbf{x}')d\mathbf{x}'$, where (see line 3 in Alg. 3) the birth density at $k-1$, i.e. $b_{k-1}(\mathbf{x}')$ is designed using the

measurements in \mathbf{Z}_{k-1} . This is done by drawing N_m particles for each $\mathbf{z} \in \mathbf{Z}_{k-1}$, hence $B_{k-1} = |\mathbf{Z}_{k-1}| \cdot N_m$. The weights of these “new-born” particles are set to $1/B_{k-1}$. The number of particles from step 5 onwards is $N + B_{k-1}$, and reduces back to N only by the resampling step (lines 13-16).

Algorithm 3 Pseudo-code of a Bernoulli bootstrap-type particle filter

```

1: function BERNOULLI PARTICLE FILTER
2:   Input:  $r_{k-1|k-1}$ ,  $\{\mathbf{x}_{k-1}^{(i)}\}_{1 \leq i \leq N}$ ,  $\mathbf{Z}_k$ ,  $\mathbf{Z}_{k-1}$ 
3:   Draw:  $\mathbf{x}_{k-1}^{(i)} \sim b_{k-1}(\mathbf{x})$  designed based on  $\mathbf{Z}_{k-1}$  for  $i = N+1, \dots, N+B_{k-1}$ 
4:   Compute the predicted existence  $r_{k|k-1}$  using (41)
5:   Draw a sample:  $\mathbf{x}_{k|k-1}^{(i)} \sim \pi_{k|k-1}(\mathbf{x}_k | \mathbf{x}_{k-1}^{(i)})$  for  $i = 1, \dots, N+B_{k-1}$ 
6:   Weights:  $w_{k|k-1}^{(i)} = \frac{p_s r_{k-1|k-1}}{N r_{k|k-1}}$  for  $i = 1, \dots, N$  ▷ 2nd term in (42)
7:   Weights:  $w_{k|k-1}^{(i)} = \frac{p_b(1-r_{k-1|k-1})}{B_{k-1} r_{k|k-1}}$  for  $i = N+1, \dots, N+B_{k-1}$  ▷ 1st term in (42)
8:   For every  $\mathbf{z} \in \mathbf{Z}_k$  compute  $I_k(\mathbf{z}) = \sum_{i=1}^{N+B_{k-1}} w_{k|k-1}^{(i)} \cdot g_k(\mathbf{z} | \mathbf{x}_{k|k-1}^{(i)})$ 
9:   Compute  $\delta_k \approx p_D \left(1 - \sum_{\mathbf{z} \in \mathbf{Z}_k} \frac{I_k(\mathbf{z})}{\lambda c(\mathbf{z})}\right)$  ▷ Eq.(45)
10:  Compute the updated existence  $r_{k|k}$  using (43)
11:  Weights:  $\tilde{w}_{k|k}^{(i)} \approx \left[1 - p_D + p_D \sum_{\mathbf{z} \in \mathbf{Z}_k} \frac{g_k(\mathbf{z} | \mathbf{x}_{k|k-1}^{(i)})}{\lambda c(\mathbf{z})}\right] \cdot w_{k|k-1}^{(i)}$ , for  $i = 1, \dots, N+B_{k-1}$ 
12:  Normalise weights:  $w_{k|k}^{(i)} = \frac{\tilde{w}_{k|k}^{(i)}}{\sum_{j=1}^{N+B_{k-1}} \tilde{w}_{k|k}^{(j)}}$ , for  $i = 1, \dots, N+B_{k-1}$ 
13:  for  $i = 1, \dots, N$  do ▷ (Resampling)
14:    Select index  $j^i \in \{1, \dots, N+B_{k-1}\}$  with probability  $w_{k|k}^{(j^i)}$ 
15:     $\mathbf{x}_k^{(i)} = \mathbf{x}_{k|k-1}^{(j^i)}$ 
16:  end for
17:  Apply MCMC move to particles and output:  $r_{k|k}$ ,  $\{\mathbf{x}_k^{(i)}\}_{1 \leq i \leq N}$ 
18: end function

```

4.4. Demonstration: Bearings-only detection and tracking

Let us demonstrate the Bernoulli particle filter in action. The observer-target scenario is the same as described in Sec. 2.4, however, this time we consider the full observation interval from $t = 0$ to $t = 3000$ [s]. Recall that the target exists only for $200[\text{s}] \leq t \leq 2400[\text{s}]$. Furthermore, detection probability is $p_D = 0.95$ and the average number of false bearings-only measurements is $\lambda = 1$ per scan. Clutter distribution is uniform, that is $c(z) = (2\pi)^{-1}[\text{rad}^{-1}]$. The parameters of the Bernoulli PF were set to: $N_m = 2500$, $p_b = 0.01$, $p_s = 0.98$. The remaining parameters were the same as in Sec. 2.4: $\sigma_w = 0.3^\circ$, $T = 20[\text{s}]$, $\sigma_v = 0.005 [\text{m/s}^2]$, $r_{\max} = 10000[\text{m}]$, $N = 5000$ particles.

Birth density $b_{k-1}(\mathbf{x})$ is designed adaptively using \mathbf{Z}_{k-1} , to form a mixture

density:

$$b_{k-1}(\mathbf{x}|\mathbf{Z}_{k-1}) = \frac{1}{|\mathbf{Z}_{k-1}|} \sum_{\mathbf{z} \in \mathbf{Z}_{k-1}} \beta(\mathbf{x}|\mathbf{z}) \quad (46)$$

Here $\beta(\mathbf{x}|\mathbf{z})$ is the birth density created using the standard technique for particle filter initialisation when tracking with bearings-only measurements, explained already in Sec. 2.4.

Fig. 2 shows the results obtained by averaging over 100 Monte Carlo runs of the Bernoulli particle filter. Fig. 2.(a) displays the average estimated probability of existence $r_{k|k}$, versus time. The true existence is indicated by the dashed blue line. Figs. 2.(b) and (c) present the RMS errors in estimated target position and velocity, respectively. The EAP estimates were computed from $\{\mathbf{x}_k^{(i)}\}_{1 \leq i \leq N}$ only at time steps when $r_{k|k} > 0.2$. The dashed blue lines in Figs. 2.(b) and (c) are the copies of the corresponding RMS errors, obtained in Sec. 2.4 (see Fig. 1) using the standard particle filter under ideal conditions (i.e. with perfect knowledge of target existence and measurements obtained with perfect detection, that is with $p_D = 1$, $\lambda = 0$). Overall, we can observe a remarkably accurate performance of the Bernoulli particle filter: it is only marginally worse than the performance under ideal conditions.

5. PHD particle filters

The RFS Bayes-optimal filter propagates the multi-object PDF $f_{k|k}(\mathbf{X}_k|\mathbf{Z}_{1:k})$, defined on the space $\mathcal{F}(\mathcal{X})$ of finite subsets of the single-object space \mathcal{X} . Since even for a relatively small number of objects it becomes cumbersome to work on $\mathcal{F}(\mathcal{X})$, several principled approximations of the RFS Bayes-optimal filter have been proposed in the context of various measurement models. The most popular among them is the probability hypothesis density (PHD) filter, derived by Mahler for the standard measurement model in [38]. Instead of propagating the posterior multi-object PDF of \mathbf{X}_k over time, the PHD filter propagates its first-order statistical moment: the intensity function or PHD (see (25)), which is defined on the space \mathcal{X} . As a simple and fast multi-object Bayes (sub-optimal) filter, whose computational complexity grows (only) linearly with the number of objects, the PHD filter has quickly become very popular among researchers. This resulted in numerous practical applications, such as passive radar [39], sonar [40], computer vision [41], traffic monitoring and road mapping [42, 43], robotic navigation and mapping [45, 46], cell microscopy [47], to name a few.

The intensity function is in general a very crude approximation of the multi-object PDF. (Recall, the multi-object PDF can be recovered from its intensity

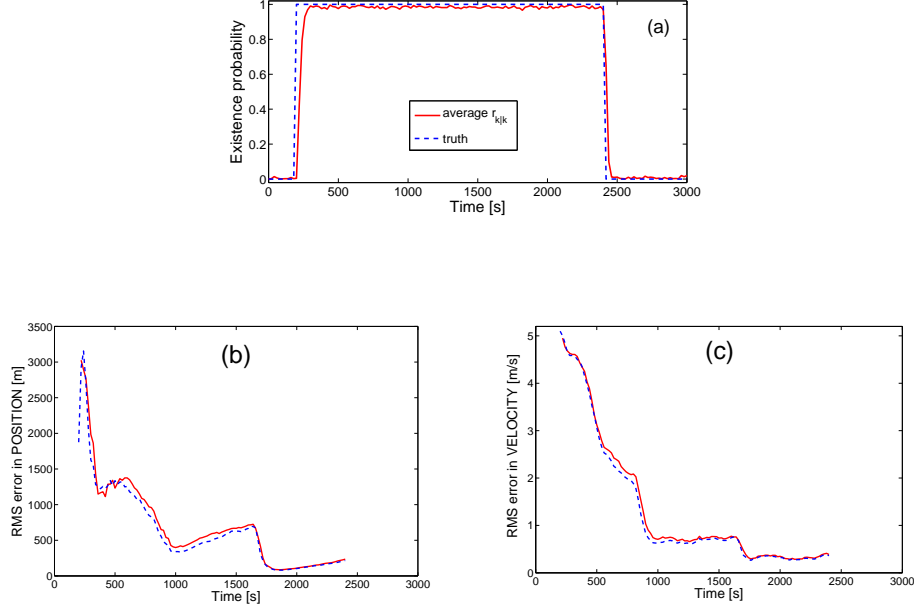


Figure 2: Bernoulli particle filter for joint detection and tracking using bearings-only measurements ($p_D = 0.95$; uniformly distributed clutter with $\lambda = 1$ per scan; $\sigma_w = 0.3^\circ$): (a) average probability of existence $r_{k|k}$ (dashed line is ideal); (b) RMS error in position; (c) RMS error in velocity (the dashed lines in (b) and (c) are the copies from Fig. 1, obtained with $p_D = 1$ and $\lambda = 0$).

function only for a Poisson RFS). Hence Mahler subsequently introduced the Cardinalised PHD filter [48], which propagates jointly the intensity function and the cardinality distribution of the multi-object PDF. The Cardinalised PHD filter improves both the estimate of the number of objects and the accuracy of the individual state estimates [49], but comes at an increased complexity. In this paper we focus only on the PHD particle filter for the standard measurement model.

5.1. Formulation of the PHD filter

The posterior intensity function (the posterior PHD) at time k , $D_{k|k}(\mathbf{x}|\mathbf{Z}_{1:k})$, is abbreviated for simplicity to $D_{k|k}(\mathbf{x})$. Recall from Sec. 3.1 that the expected number of objects present at time k can be estimated from $D_{k|k}(\mathbf{x})$ as $\nu_{k|k} = \int_{\mathcal{X}} D_{k|k}(\mathbf{x}) d\mathbf{x}$, where $\nu_{k|k} \in \mathbb{R}$.

Assuming that the PHD function at $k-1$ is available, the prediction equation

of the PHD filter is given by [38]:

$$D_{k|k-1}(\mathbf{x}) = \gamma_{k|k-1}(\mathbf{x}) + p_s \int \pi_{k|k-1}(\mathbf{x}|\mathbf{x}') D_{k-1|k-1}(\mathbf{x}') d\mathbf{x}' \quad (47)$$

where $\gamma_{k|k-1}(\mathbf{x})$ is the PHD of the RFS of object births between time $k-1$ and k . Following the measurement-driven design of the birth density in Sec. 4.3, we model $\gamma_{k|k-1}(\mathbf{x}) = p_s \int \pi_{k|k-1}(\mathbf{x}|\mathbf{x}') \gamma_{k-1}(\mathbf{x}') d\mathbf{x}'$, where assuming a Poisson birth RFS, $\gamma_{k-1}(\mathbf{x}) = \nu_b b_{k-1}(\mathbf{x}|\mathbf{Z}_{k-1})$. Here ν_b is the expected number of object births between time $k-1$ and k (a design parameter, typically small, e.g. 0.1) and $b_{k-1}(\mathbf{x}|\mathbf{Z}_{k-1})$ is the birth density (46).

Upon receiving the measurement set \mathbf{Z}_k at time k , the update step of the PHD filter is computed according to:

$$D_{k|k}(\mathbf{x}) = \left[1 - p_D + \sum_{\mathbf{z} \in \mathbf{Z}_k} \frac{p_D g_k(\mathbf{z}|\mathbf{x})}{\kappa_k(\mathbf{z}) + p_D \int g_k(\mathbf{z}|\mathbf{x}) D_{k|k-1}(\mathbf{x}) d\mathbf{x}} \right] D_{k|k-1}(\mathbf{x}) \quad (48)$$

where $\kappa_k(\mathbf{z})$ is the PHD of the clutter RFS at time k . Assuming clutter is a Poisson RFS, see (35), its PHD is $\kappa_k(\mathbf{z}) = \lambda c(\mathbf{z})$. Note that in (48) for simplicity we assume that the probability of detection p_D is independent of the state. The case $p_D(\mathbf{x})$ is a straightforward generalisation.

It can be easily verified that in the absence of clutter and target birth, with $\mathbf{Z}_k = \{\mathbf{z}\}$, $p_s = p_D = 1$, the PHD filter equations (47)-(48) reduce to the standard Bayes filter equations (3)-(4).

The PHD filter recursion (47)-(48) is initialised with $D_{0|0}(\mathbf{x})$. In the absence of any prior, we can set $D_{0|0}(\mathbf{x}) = 0$, meaning that initially there are no objects in the surveillance volume.

5.2. The particle method applied to PHD filtering

In the general nonlinear/non-Gaussian context, the PHD filter cannot be solved analytically, and is typically implemented using the particle method. The conceptual framework for an efficient particle PHD filter implementation has been cast in [28], where the proposal (importance) densities for drawing particles need to depend on the latest measurement set \mathbf{Z}_k . How to construct these importance densities has been a topic of intensive research in the last decade, see [50], [49], [51], [52]. The method described below mainly follows [53].

The PHD particle filter propagates through time the particle system $\mathcal{P}_k \equiv \{w_k^{(i)}, \mathbf{x}_k^{(i)}\}_{1 \leq i \leq N_k}$, which approximates $D_{k|k}(\mathbf{x})$. Note that $w_k^{(i)} \geq 0$ and $\sum_{i=1}^{N_k} w_k^{(i)} = \hat{\nu}_{k|k} \geq 0$ is an estimate of the expected number of objects $\nu_{k|k} = \int_{\mathcal{X}} D_{k|k}(\mathbf{x}) d\mathbf{x}$.

The pseudo-code of a PHD particle filter algorithm is given in Alg. 4. This code is general enough to be used with any type of a particle filter (e.g. the auxiliary PF, the exact particle flow filter, the PF with progressive correction, see Sec. 2.2), naturally including the bootstrap filter. In addition, at each time step it produces an estimate of the multi-object state $\hat{\mathbf{X}}_k$ and, if required, the probability of existence for each $\mathbf{x} \in \hat{\mathbf{X}}_k$.

Algorithm 4 Pseudo-code of a PHD particle filter

```

1: function PHD PARTICLE FILTER
2:   Input:  $\mathcal{P}_{k-1} \equiv \{w_{k-1}^{(i)}, \mathbf{x}_{k-1}^{(i)}\}_{1 \leq i \leq N_{k-1}}, \mathbf{Z}_k, \mathbf{Z}_{k-1}$ 
3:   Draw:  $\mathbf{x}_{k-1}^{(i)} \sim b_{k-1}(\mathbf{x}|\mathbf{Z}_{k-1})$  for  $i = N_{k-1} + 1, \dots, N_{k-1} + B_{k-1}$ 
4:   Set weights:  $w_{k-1}^{(i)} = \nu_b/B_{k-1}$  for  $i = N_{k-1} + 1, \dots, N_{k-1} + B_{k-1}$ .
5:   Draw a sample:  $\mathbf{x}_{k|k-1}^{(i)} \sim \pi_{k|k-1}(\mathbf{x}_k|\mathbf{x}_{k-1}^{(i)})$  for  $i = 1, \dots, N_{k-1} + B_{k-1}$ 
6:   Predict weights:  $w_{k|k-1}^{(i)} = p_s w_{k-1}^{(i)}$  for  $i = 1, \dots, N_{k-1} + B_{k-1}$ .
7:   Partition  $\{w_{k|k-1}^{(i)}, \mathbf{x}_{k|k-1}^{(i)}\}_{1 \leq i \leq N_{k-1} + B_{k-1}}$  to form clusters  $\mathcal{C}_{k|k-1}(\mathbf{z}), \forall \mathbf{z} \in \mathbf{Z}_k \cup \emptyset$ 
8:   Initialise:  $\mathcal{P}_k = \emptyset, \hat{\mathbf{X}}_k = \emptyset$ 
9:   for every  $\mathbf{z} \in \mathbf{Z}_k$  do
10:    if  $\mathcal{C}_{k|k-1}(\mathbf{z}) \neq \emptyset$  then
11:       $\mathcal{C}_k(\mathbf{z}) = PFU[\mathcal{C}_{k|k-1}(\mathbf{z}), \mathbf{z}]$  ▷ See Alg. 5
12:       $\mathcal{P}_k = \mathcal{P}_k \cup \mathcal{C}_k(\mathbf{z})$ 
13:      Compute existence prob.  $p_e(\mathbf{z})$  for  $\mathcal{C}_k(\mathbf{z})$ 
14:      if  $p_e(\mathbf{z}) > \eta$  then, ▷  $\eta$  is reporting threshold
15:        Compute EAP estimate  $\hat{\mathbf{x}}_k$  from  $\mathcal{C}_k(\mathbf{z})$ 
16:         $\hat{\mathbf{X}}_k = \hat{\mathbf{X}}_k \cup \{\hat{\mathbf{x}}_k\}$ 
17:      end if
18:    end if
19:  end for
20:  for every pair  $(w_{k|k-1}, \mathbf{x}_{k|k-1}) \in \mathcal{C}_{k|k-1}(\emptyset)$  do
21:    if  $w_{k|k-1} > \xi$  then ▷  $\xi$  is threshold
22:       $\mathcal{P}_k = \mathcal{P}_k \cup \{(1 - p_D)w_{k|k-1}, \mathbf{x}_{k|k-1}\}$ 
23:    end if
24:  end for
25:  Output:  $\mathcal{P}_k \equiv \{w_k^{(i)}, \mathbf{x}_k^{(i)}\}_{1 \leq i \leq N_k}; \hat{\mathbf{X}}_k$ 
26: end function

```

In line 3, $B_{k-1} = N_m \cdot |\mathbf{Z}_{k-1}|$ particles, for potentially newborn targets, are drawn from the birth density $b_{k-1}(\mathbf{x}|\mathbf{Z}_{k-1})$ defined in (46). These particles, indexed by $i = N_{k-1} + 1, \dots, N_{k-1} + B_{k-1}$, are given equal weights, $w_{k-1}^{(i)} = \nu_b/B_{k-1}$ (see line 4), so that their sum is $\sum_{i=N_{k-1}+1}^{N_{k-1}+B_{k-1}} w_{k-1}^{(i)} = \nu_b$. Implementation of (47) then follows in lines 4-6: both *persistent* and *newborn* target particles are propagated through the transitional density in line 5, while their weights are multiplied by p_s (line 6).

Line 7 in Alg. 4 is very unusual and needs a detailed explanation. Previous

approaches to PHD particle filtering [28], [49] treated the term in the square brackets on the RHS of (48) as a pseudo-likelihood. Then the weights of all predicted particles, obtained after line 6, i.e. $\{w_{k|k-1}^{(i)}, \mathbf{x}_{k|k-1}^{(i)}\}_{1 \leq i \leq N_{k-1} + B_{k-1}}$ were updated directly using (48) as follows:

$$\tilde{w}_{k|k}^{(i)} = \left[1 - p_D + \sum_{\mathbf{z} \in \mathbf{Z}_k} \frac{p_D g_k(\mathbf{z} | \mathbf{x}_{k|k-1}^{(i)})}{\kappa_k(\mathbf{z}) + p_D \sum_{i=1}^{N_{k-1} + B_{k-1}} g_k(\mathbf{z} | \mathbf{x}_{k|k-1}^{(i)}) w_{k|k-1}^{(i)}} \right] w_{k|k-1}^{(i)} \quad (49)$$

for $i = 1, \dots, N_{k-1} + B_{k-1}$. This would be followed by resampling (using normalised weights) and possibly particle diversification using for example the MCMC move step. This approach, referred to as the pseudo-likelihood update (PLU), will be demonstrated for the sake of comparison. It suffers from two problems. First, the particles representing the targets that were undetected at time k would not survive the resampling step. As a result, these targets would have to be re-initialised when detected at a future time, which is very inefficient for applications such as bearings-only filtering (due to the un-observability of target range). Second, estimation of the multi-target state, i.e. $\hat{\mathbf{X}}_k$, from the particle system after the described update step would be cumbersome. The standard approach [54], [27, p.623], [9, Sec.9.6] is to first estimate the number of targets as the nearest integer value corresponding to the sum of the weights in (49), followed by partitioning of the particles using a data clustering algorithm. Finally, the mean values of the clusters of particles become the EAP estimates included in $\hat{\mathbf{X}}_k$. Various clustering algorithms have been compared, such as hierarchical clustering, k-means and the EM algorithm. Clustering in this context is completely ad-hoc and destroys the elegance of the PHD particle filter.

Alg. 4 avoids the described shortcomings. In line 7 particles are partitioned in a principled manner using the update equation (48). Note that the RHS of (48) contains $|\mathbf{Z}_k| + 1$ additive terms. For each particle-measurement pair, an additive term in the sum on the RHS of (48) can be interpreted as the probability that measurement \mathbf{z}_j , $j = 1, \dots, |\mathbf{Z}_k|$ is due to an object in the state $\mathbf{x}_{k|k-1}^{(i)}$, $i = 1, \dots, N_{k-1} + B_{k-1}$ [30, p.78]:

$$P_{ij} = \frac{p_D g_k(\mathbf{z}_j | \mathbf{x}_{k|k-1}^{(i)}) w_{k|k-1}^{(i)}}{\kappa(\mathbf{z}_j) + p_D \sum_{\ell=1}^{N_{k-1} + B_{k-1}} g_k(\mathbf{z}_j | \mathbf{x}_{k|k-1}^{(\ell)}) w_{k|k-1}^{(\ell)}}. \quad (50)$$

The remaining additive term in (48) can be interpreted as the probability that an object in the state $\mathbf{x}_{k|k-1}^{(i)}$ has not been detected. We index this case with

$j = 0$, i.e. its probability is [30, p.78]:

$$P_{i0} = (1 - p_D) w_{k|k-1}^{(i)}. \quad (51)$$

It can be easily verified that $0 \leq P_{ij} \leq 1$ for all $j = 0, \dots, |\mathbf{Z}_k|$.

Partitioning of $\mathcal{P}_{k|k-1} \equiv \{w_{k|k-1}^{(i)}, \mathbf{x}_{k|k-1}^{(i)}\}_{1 \leq i \leq N_{k-1} + B_{k-1}}$ now proceeds based on (50) and (51). For a particle with index i in $\mathcal{P}_{k|k-1}$, one can compute the probability distribution over the elements of \mathbf{Z}_k , plus the empty set, as follows

$$p_i(j) = \frac{P_{ij}}{\sum_{\ell=0}^{|\mathbf{Z}_k|} P_{i\ell}}, \quad j = 0, 1, \dots, |\mathbf{Z}_k|. \quad (52)$$

Partitioning of particles in $\mathcal{P}_{k|k-1}$ is next carried out in a probabilistic manner as follows. For each $i = 1, \dots, N_{k-1} + B_{k-1}$ we select an index $j^i \in \{0, 1, \dots, |\mathbf{Z}_k|\}$ with probability $p_i(j)$. The weighted particle $(w_{k|k-1}^{(i)}, \mathbf{x}_{k|k-1}^{(i)})$ from $\mathcal{P}_{k|k-1}$ is then assigned to cluster $\mathcal{C}_{k+1|k}(\mathbf{z}_{j^i})$. When this procedure is complete we end up with $|\mathbf{Z}_k| + 1$ clusters $\mathcal{C}_{k+1|k}(\mathbf{z})$, $\forall \mathbf{z} \in \mathbf{Z}_k \cup \emptyset$. Note that some of the clusters may end up being empty (for example, if $\mathbf{z} \in \mathbf{Z}_k$ is a false detection, $\mathcal{C}_{k|k-1}(\mathbf{z})$ is likely to be empty).

Processing steps from line 9 to line 24 in Alg. 4 are self-explanatory, except for line 11. Let us denote a component of $D_{k|k-1}(\mathbf{x})$ which is approximated by the particles in cluster $\mathcal{C}_{k|k-1}(\mathbf{z}_j)$ by $D_{k|k-1}^j(\mathbf{x})$. According to (48), the Bayes update of $D_{k|k-1}^j(\mathbf{x})$ using the assigned measurement $\mathbf{z}_j \in \mathbf{Z}_k$ is as follows:

$$D_k^j(\mathbf{x}) = \frac{p_D g_k(\mathbf{z}_j|\mathbf{x}) D_{k|k-1}^j(\mathbf{x})}{\kappa(\mathbf{z}_j) + p_D \int g_k(\mathbf{z}_j|\mathbf{x}) D_{k|k-1}^j(\mathbf{x}) d\mathbf{x}} \quad (53)$$

A slight modification of any standard particle filter can implement (53). This step is carried out in line 11 where PFU stands for *particle-filter update* (to be explained later). The output of the PFU based on $\mathbf{z} \in \mathbf{Z}_k$ is a cluster $\mathcal{C}_k(\mathbf{z}) = \{w_k^{(\ell)}, \mathbf{x}_k^{(\ell)}\}_{1 \leq \ell \leq L}$, which is added to the particle system \mathcal{P}_k in line 12. The sum of the updated weights in cluster $\mathcal{C}_k(\mathbf{z})$ is less than or equal to 1 and represents the probability of existence p_e (i.e. the probability that a target, whose posterior PDF is approximated by $\mathcal{C}_k(\mathbf{z})$, exists). The probability of existence is computed in line 13, and then in line 14 compared to the reporting threshold η . If p_e is above this threshold, an EAP estimate is computed using cluster $\mathcal{C}_k(\mathbf{z})$, see line 15, to be subsequently included in the multi-object state estimate $\hat{\mathbf{X}}_k$, see line 16.

The particles of cluster $\mathcal{C}_{k|k-1}(\emptyset)$ have not been assigned any measurement for the update, and therefore are treated differently (see the loop between lines 20 and 24). Recall that every measurement induces the so-called newborn target

particles. If unchecked, this could potentially result in an ever-growing number of particles over time. The if-then clause in line 21 of Alg. 4 is introduced to prevent that from happening. The particles in cluster $\mathcal{C}_{k|k-1}(\emptyset)$ whose weights are smaller than threshold ξ are eliminated and therefore cannot propagate further in time (e.g. those initially induced on false detections, or those corresponding to targets that ceased to exist). The particle elimination threshold ξ (line 21) must be chosen so that the particles on undetected but currently present (existing) objects are not eliminated. This is particularly important in applications such as bearings-only tracking, where target range is initially unobservable.

The bootstrap-type PFU (line 11 in Alg. 4) is described by pseudo-code in Alg. 5. A PFU routine based on progressive correction is discussed in [53]. Let the cluster $\mathcal{C}_{k|k-1}(\mathbf{z})$ consist of M weighted particles, $\{w_{k|k-1}^{(m)}, \mathbf{x}_{k|k-1}^{(m)}\}_{1 \leq m \leq M}$. According to (53), the weight of a predicted particle $\mathbf{x}_{k|k-1}^{(m)}$ from $\mathcal{C}_{k|k-1}(\mathbf{z})$ is updated as:

$$\tilde{w}_k^{(m)} = \frac{p_D g_k(\mathbf{z} | \mathbf{x}_{k|k-1}^{(m)}) w_{k|k-1}^{(m)}}{\kappa(\mathbf{z}) + p_D \sum_{j=1}^M g_k(\mathbf{z} | \mathbf{x}_{k|k-1}^{(j)}) w_{k|k-1}^{(j)}} \quad (54)$$

This step is carried out in line 4 of Alg. 5, followed by resampling (using normalised weights), see the loop between lines 7 and 11. While the number of particles M in the input cluster $\mathcal{C}_{k|k-1}(\mathbf{z})$ varies from cluster to cluster, resampling (line 7) is always carried out L times, where L is a user-defined parameter. Note from line 10 (Alg. 5) that the probability of cluster existence p_e remains unchanged by the PFU routine.

Algorithm 5 Bootstrap-type PFU (line 11 of Alg. 4)

```

1: function BOOTSTRAP-TYPE PFU
2:   Input:  $\mathcal{C}_{k|k-1}(\mathbf{z}) = \{w_{k|k-1}^{(m)}, \mathbf{x}_{k|k-1}^{(m)}\}_{m=1}^M, \mathbf{z}$ 
3:   for  $m = 1, \dots, M$  do
4:     Compute  $\tilde{w}_k^{(m)}$  according to (54)
5:   end for
6:   Compute  $p_e = \sum_{m=1}^M \tilde{w}_k^{(m)}$ 
7:   for  $\ell = 1, \dots, L$  do ▷ Resampling loop
8:     Select  $c \in \{1, \dots, M\}$  with prob.  $\tilde{w}_k^{(c)} / p_e$ 
9:      $\mathbf{x}_k^{(\ell)} \leftarrow \mathbf{x}_{k|k-1}^{(c)}$ 
10:     $w_k^{(\ell)} = p_e / L$ 
11:  end for
12:  Output: Apply MCMC move and output  $\mathcal{C}_k = \{w_k^{(\ell)}, \mathbf{x}_k^{(\ell)}\}_{\ell=1}^L$ 
13: end function

```

5.3. Calibration of tracking algorithms

Tracking algorithms are based on mathematical models, in particular the dynamic model (for target birth/survival and motion) and the sensor measurement model. These models typically include many parameters, such as the target birth rate ν_b , survival probability p_s , the false alarm rate λ , the probability of detection p_D , measurement noise variance, but also sensor biases, various factors such as the propagation losses, receiver gains, etc. Calibration of tracking algorithms, through estimation of their model parameters, is an important prerequisite for their operational deployment.

In accordance with Sec. 2.3, let a random vector $\boldsymbol{\theta} \in \boldsymbol{\Theta} \subset \mathcal{R}^{n_\theta}$ represent the static parameter vector of interest for estimation/calibration. Again we will indicate this in notation as $\Pi_{k|k-1}(\mathbf{X}_k|\mathbf{X}_{k-1}, \boldsymbol{\theta})$, for the FISST transitional density and $\varphi_k(\mathbf{Z}_k|\mathbf{X}_k, \boldsymbol{\theta})$, for the FISST likelihood function. The problem is to estimate the posterior density $p(\boldsymbol{\theta}|\mathbf{Z}_{1:k}) \propto \varrho(\mathbf{Z}_{1:k}|\boldsymbol{\theta})p(\boldsymbol{\theta})$, given the prior $p(\boldsymbol{\theta})$. Similarly to the arguments presented in Sec. 2.3, the complicating factor is that the likelihood function $\varrho(\mathbf{Z}_{1:k}|\boldsymbol{\theta})$ cannot be expressed in closed-form. However, note that, similar to (8), we can apply a decomposition:

$$\varrho(\mathbf{Z}_{1:k}|\boldsymbol{\theta}) = \varrho(\mathbf{Z}|\boldsymbol{\theta}) \prod_{t=2}^k \varrho(\mathbf{Z}_t|\mathbf{Z}_{1:t-1}, \boldsymbol{\theta})$$

where

$$\varrho(\mathbf{Z}_t|\mathbf{Z}_{1:t-1}, \boldsymbol{\theta}) = \int \varphi_k(\mathbf{Z}_k|\mathbf{X}_k, \boldsymbol{\theta}) f(\mathbf{X}_k|\mathbf{Z}_{1:k-1}, \boldsymbol{\theta}) \delta \mathbf{X}_k$$

The key observation here is that the conditional likelihood $\varrho(\mathbf{Z}_t|\mathbf{Z}_{1:t-1}, \boldsymbol{\theta})$ can be computed as a by-product of the PHD filter, see [38, Eq.(116)]:

$$\begin{aligned} \varrho(\mathbf{Z}_k|\mathbf{Z}_{1:k-1}, \boldsymbol{\theta}) &\propto \exp \left\{ -p_D(\boldsymbol{\theta}) \int D_{k|k-1}(\mathbf{x}|\mathbf{Z}_{1:k-1}, \boldsymbol{\theta}) d\mathbf{x} \right\} \times \\ &\prod_{\mathbf{z} \in \mathbf{Z}_k} \left(\kappa(\mathbf{z}|\boldsymbol{\theta}) + p_D(\boldsymbol{\theta}) \int g_k(\mathbf{z}|\mathbf{x}, \boldsymbol{\theta}) D_{k|k-1}(\mathbf{x}|\mathbf{Z}_{1:k-1}, \boldsymbol{\theta}) d\mathbf{x} \right) \end{aligned} \quad (55)$$

Using the PHD particle filter, (55) can be estimated from the particle system $\mathcal{P}_{k|k-1} \equiv \{w_{k|k-1}^{(i)}, \mathbf{x}_{k|k-1}^{(i)}\}_{1 \leq i \leq N_{k-1} + B_{k-1}}$, available after line 6 in Alg. 4, as

follows:

$$\begin{aligned} \widehat{\ell}(\mathbf{Z}_k | \mathbf{Z}_{1:k-1}, \boldsymbol{\theta}) \propto \exp \left\{ -p_D(\boldsymbol{\theta}) \sum_{i=1}^{N_{k-1}+B_{k-1}} w_{k|k-1}^{(i)} \right\} \times \\ \prod_{\mathbf{z} \in \mathbf{Z}_k} \left(\kappa(\mathbf{z} | \boldsymbol{\theta}) + p_D(\boldsymbol{\theta}) \sum_{i=1}^{N_{k-1}+B_{k-1}} g_k(\mathbf{z} | \mathbf{x}_{k|k-1}^{(i)}, \boldsymbol{\theta}) w_{k|k-1}^{(i)} \right) \end{aligned} \quad (56)$$

Now one can apply any of the standard Monte Carlo parameter estimation algorithms (e.g. MCMC) to estimate the posterior $p(\boldsymbol{\theta} | \mathbf{Z}_{1:K})$. Note that in every MCMC iteration, for the proposed value of $\boldsymbol{\theta}$, it is necessary to run the PHD particle filter in order to compute (56). The factor of proportionality in (56) cancels out and hence is irrelevant.

The described method has been demonstrated in the context of sensor bias calibration, see [55]. However, its impact is much broader. Suppose the calibration parameter is a stochastic dynamic process whose evolution is independent of \mathbf{X}_k . Then based on the factorization of the posterior PHD function: $D_{k|k}(\mathbf{x}_k, \boldsymbol{\theta}_k | \mathbf{Z}_{1:k}) = D_{k|k}(\mathbf{x}_k | \boldsymbol{\theta}_k, \mathbf{Z}_{1:k}) p_{k|k}(\boldsymbol{\theta}_k | \mathbf{Z}_{1:k})$, one can apply a hierarchical particle method as follows: the standard particle filter on the $\boldsymbol{\Theta}$ space, and the PHD particle filter on the $\mathcal{X} | \boldsymbol{\Theta}$ space. This approach was demonstrated in the context of joint tracking and time-varying bias estimation in [56]. Moreover, if $D_{k|k}(\mathbf{x}_k | \boldsymbol{\theta}_k, \mathbf{Z}_{1:k})$ is analytically tractable (e.g. linear/Gaussian target tracking), then one can effectively apply a Rao-Blackwellised formulation. This is the essence of the algorithms proposed for: tracking groups of targets [57], tracking an extended target [58] and simultaneous localisation and mapping (SLAM) [44, 46, 59].

5.4. Demonstration: Bearings-only multi-object filtering

The performance of the described PHD particle filter is demonstrated using the simulated scenario taken from [26], which consist of four targets and lasts 3000[s]. The geometry is shown in Fig. 3.(a). The circles on each trajectory indicate the starting points. One target is present at the beginning, with another three arriving during the first 400[s]. Three targets are terminating in the final 900[s]. The bearings of all four targets cross one another in the middle of the observation interval. We assume an ideal sensor with infinite resolution.

In order to measure the statistical error of multi-object filtering at each time step we need a distance metric between two finite sets of objects: the ground truth \mathbf{X}_k and its estimate $\widehat{\mathbf{X}}_k$. The optimal subpattern assignment (OSPA)

distance [60] has become a widespread metric for this purpose as it captures both the difference in the cardinality of the two finite sets and the positional error of their respective elements. The OSPA distance has two parameters: (1) the cut-off value, which we adopt as $c = 5[\text{km}]$; (2) the order parameter of the Euclidian base distance (in position), which we adopt as $p = 2$.

Fig. 3.(b) shows the OSPA error averaged over 500 Monte Carlo runs, for two PHD particle filters: the one described by Algs. 4 and 5, and the alternative, based on the pseudo-likelihood update step [49]. The parameters used in simulations were: $p_D = 0.95$; Poisson clutter with $\lambda = 1$ and $c(z) = (2\pi)^{-1}[\text{rad}^{-1}]$; $N_m = 2500$, $p_b = 0.01$, $p_s = 0.98$; $\sigma_w = 1^\circ$, $T = 20[\text{s}]$, $\sigma_v = 0.005 [\text{m/s}^2]$, $r_{\max} = 10000[\text{m}]$, and $N = 5000$ particles. Clearly, the PHD particle filter described by Algs. 4 and 5, which includes the partitioning of particles, performs much better than the alternative based on PLU.

6. Labelled RFS Bayes tracking filters

Since the introduction of RFS Bayes filters (optimal and suboptimal), there have been numerous attempts to apply them to multi-target tracking problems, e.g. [54], [61], [41], [62]. These heuristic methods typically label the targets and apply some form of data association to keep track of the labels as time progresses. Mahler's view [27] was that the most natural and therefore convenient RFS for multi-target tracking is the multi-Bernoulli RFS, introduced in Sec. 3.2. His initial formulation led to the development of an approximation of the RFS Bayes-optimal filter referred to as the CBMeMBer filter [63]. Assuming the multi-object PDF $f_{k|k}(\mathbf{X}_k|\mathbf{Z}_{1:k})$ is multi-Bernoulli, the CBMeMBer filter propagates the pairs $(r_{k|k}^j, p_{k|k}^j(\mathbf{x}))$, $j = 1, \dots, M_k$ over time via the prediction and update steps. While the prediction step (36) for the CBMeMBer filter can be derived in closed-form exactly, the update step (37) formulation is based on a (fairly un-intuitive) approximation.

The breakthrough was made in [64] with the formulation of *labelled* random finite sets. While preserving the mathematical rigor of the RFS framework, the labelled RFS concept allows the assignment of a distinct label to each object (target) that appears in the surveillance volume during the observation time. The history of the state evolution for each object (i.e. its trajectory) can then be naturally identified. More importantly, this framework allows the formulation of an exact closed-form Bayes-optimal multi-target tracking filter [65]. Related relevant recent papers include [66, 67].

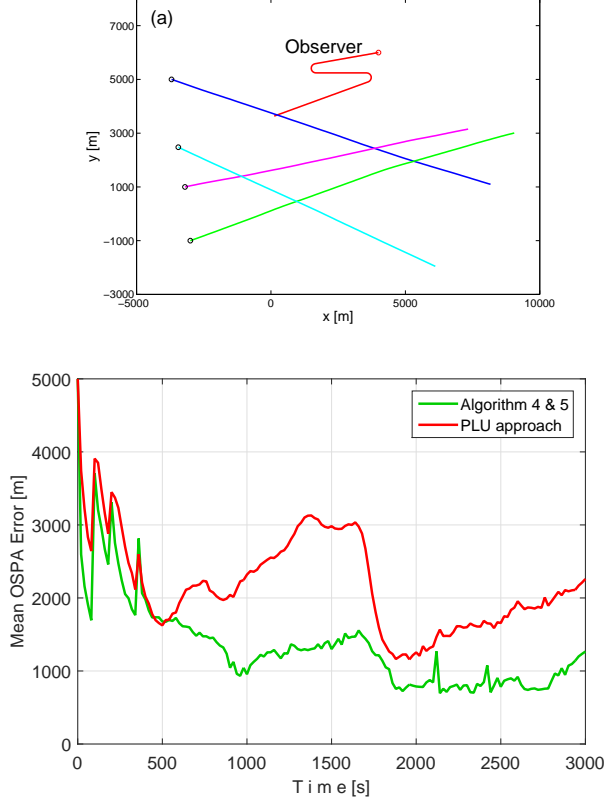


Figure 3: Bearings-only multi-target filtering results: (a) the simulated scenario (observer and four targets, circles indicating the starting points); (b) The mean OSPA error (which captures both the cardinality error and the positional error) for two PHD particle filters.

6.1. Labelled RFS

Suppose the elements of an RFS \mathbb{X} on \mathcal{X} are uniquely tagged by an (unobserved) label drawn from a discrete countable space of labels \mathcal{L} . A labelled RFS, denoted \mathbb{X} , is an RFS on the product space $\mathcal{X} \times \mathcal{L}$, such that each realisation of \mathbb{X} has distinct labels. We express distinctness of labels mathematically by introducing the *distinct label indicator* function $\Delta(\mathbb{X})$. Specifically, if we assume that $\mathbb{X} = \{(\mathbf{x}_1, \ell_1), \dots, (\mathbf{x}_n, \ell_n)\}$, then the distinct label indicator is defined as

$$\Delta(\mathbb{X}) = \delta[|\mathbb{X}|, |\mathfrak{L}_{\mathbb{X}}|],$$

where $\mathfrak{L}_{\mathbb{X}} = \{\ell_1, \dots, \ell_n\}$ is the set of unique labels in \mathbb{X} and $\delta[a, b]$ is the Kronecker delta function, defined earlier. By definition, a realisation of a labelled RFS \mathbb{X} always satisfies $\Delta(\mathbb{X}) = 1$. Labelled RFSs include, for example, the

labelled Poisson RFS, and the labelled multi-Bernoulli RFS, see [64]. In order to distinguish the distributions and statistics of labelled versus unlabelled random variables (both vectors and finite sets), functions of labelled random variables will be denoted with a tilde sign. For example, a PDF on the space $\mathcal{X} \times \mathcal{L}$ is denoted \tilde{p} , while a PDF on $\mathcal{F}(\mathcal{X} \times \mathcal{L})$ is denoted \tilde{f} .

For an analytical formulation of the RFS Bayes optimal tracking filter, of particular interest is a general class of labelled RFS, referred to as the *generalised labelled multi-Bernoulli* (GLMB) RFS [64]. The PDF of a GLMB RFS \mathbb{X} , with single object state space \mathcal{X} and discrete-label space \mathcal{L} is given by:

$$\tilde{f}(\mathbb{X}) = \Delta(\mathbb{X}) \sum_{j \in J} \phi^j(\mathfrak{L}_{\mathbb{X}}) \prod_{(\mathbf{x}, \ell) \in \mathbb{X}} \tilde{p}^j(\mathbf{x}, \ell) \quad (57)$$

where J is an arbitrary index set, and ϕ^j and \tilde{p}^j satisfy

$$\sum_{L \subseteq \mathcal{L}} \sum_{j \in J} \phi^j(L) = 1 \text{ and } \int_{\mathbf{x} \in \mathcal{X}} \tilde{p}^j(\mathbf{x}, \ell) d\mathbf{x} = 1, \forall \ell \in \mathcal{L}.$$

This RFS has a remarkable property that its PDF is a conjugate prior for the standard multi-object likelihood function (34) and is closed under the Chapman-Kolmogorov prediction with the standard multi-object transitional model.

The GLMB is a very general and flexible RFS model, but its application to multi-target tracking problems is more easily demonstrated by considering a more specific type of GLMB RFS, which was also proposed in [64]. A δ -generalised labelled multi-Bernoulli (δ -GLMB) RFS with state space \mathcal{X} and label space \mathcal{L} , is a GLMB RFS with density of the same form as (57), with the following substitutions

$$J = \mathcal{F}(\mathcal{L}) \times \Xi, \quad (58)$$

$$\phi^j(L) = \phi^{I, \xi}(L) = \phi^{I, \xi} \delta[I, L], \quad (59)$$

$$\tilde{p}^j = \tilde{p}^{I, \xi} = \tilde{p}^{\xi}, \quad (60)$$

where $\delta[X, Y]$ is a generalisation of the Kroneker delta for sets (i.e. $\delta[X, Y] = 1$ if $X = Y$ and zero otherwise), and Ξ is a discrete space. Thus, a δ -GLMB RFS is distributed according to

$$\tilde{f}(\mathbb{X}) = \Delta(\mathbb{X}) \sum_{(I, \xi) \in \mathcal{F}(\mathcal{L}) \times \Xi} \phi^{I, \xi} \delta[I, \mathfrak{L}_{\mathbb{X}}] \prod_{(\mathbf{x}, \ell) \in \mathbb{X}} \tilde{p}^{\xi}(\mathbf{x}, \ell). \quad (61)$$

In a δ -GLMB, the sum is taken over the Cartesian product between the space of finite subsets of \mathcal{L} , and the discrete space Ξ . In tracking applications, each subset of \mathcal{L} represents a set of target labels, while Ξ represents the space of

measurement-to-label association histories. Hence, a particular element $(I, \xi) \in \mathcal{F}(\mathcal{L}) \times \Xi$ can be considered to be the hypothesis that the set of currently existing targets are those with labels I and association history ξ . The weight $\phi^{I, \xi}$ is the probability of this hypothesis, and $\tilde{p}^\xi(\mathbf{x}, \ell)$ is the PDF of the target with label ℓ under the association history ξ .

Like the GLMB, the δ -GLMB has also been shown to be closed under the standard multi-object prediction, and a conjugate prior with respect to the standard multi-object measurement likelihood [64]. This makes the δ -GLMB a highly useful tool for deriving analytical Bayes recursions for multi-object tracking problems.

6.2. Labelled multi-object transition and likelihood models

The labelled version of the likelihood model $\varphi_k(\mathbf{Z}|\mathbb{X})$ essentially has the same form as (34), with only a few notes of caution. First, the probability of detection is assumed to depend on the state of the target and its label, and therefore p_D in (34) should be replaced with $\tilde{p}_D(\mathbf{x}, \ell)$. Second, a target-to-measurement association is defined as a mapping $\theta : \mathcal{L}_\mathbb{X} \rightarrow \{0, 1, \dots, |\mathbf{Z}|\}$. Finally, in the context of labelled RFSs, we need to substitute \mathbf{x}_i and \mathbf{X} in (34) with (\mathbf{x}_i, ℓ_i) and \mathbb{X} , respectively.

The labelled version of the standard multi-target dynamic model is more involved. Let \mathbb{X} be the labelled RFS of objects at the current time with label space \mathcal{L} . A particular object $(\mathbf{x}, \ell) \in \mathbb{X}$ has probability $\tilde{p}_s(\mathbf{x}, \ell)$ of surviving to the next time with state (\mathbf{x}_+, ℓ_+) and probability density $\pi(\mathbf{x}_+|\mathbf{x}, \ell) \delta[\ell, \ell_+]$ (where $\pi(\mathbf{x}_+|\mathbf{x}, \ell)$ is the single target transition kernel), and probability, $1 - \tilde{p}_s(\mathbf{x}, \ell)$ of being terminated. Thus, the set \mathbb{S} of surviving objects at the next time is distributed according to

$$\tilde{\Pi}_S(\mathbb{S}|\mathbb{X}) = \Delta(\mathbb{S}) \Delta(\mathbb{X}) 1_{\mathcal{L}_\mathbb{X}}(\mathcal{L}_\mathbb{S}) \prod_{(\mathbf{x}, \ell) \in \mathbb{X}} \tilde{\Phi}(\mathbb{S}; \mathbf{x}, \ell), \quad (62)$$

where $1_A(B)$ is a generalisation of the indicator function for sets, such that $1_A(B) = 1$ if $B \subseteq A$ and zero otherwise, and

$$\tilde{\Phi}(\mathbb{S}; \mathbf{x}, \ell) = \begin{cases} \tilde{p}_s(\mathbf{x}, \ell) \pi(\mathbf{x}_+|\mathbf{x}, \ell), & \text{if } \ell \in \mathcal{L}_\mathbb{S} \\ 1 - \tilde{p}_s(\mathbf{x}, \ell), & \text{if } \ell \notin \mathcal{L}_\mathbb{S} \end{cases} \quad (63)$$

Let \mathbb{B} be the labelled RFS of newborn objects with label space \mathcal{B} , where $\mathcal{L} \cap \mathcal{B} = \emptyset$. Since the births have distinct labels, and assuming that their states are independent, we model \mathbb{B} as a labelled multi-Bernoulli (LMB) RFS, which

is distributed according to

$$\tilde{f}_b(\mathbb{B}) = \Delta(\mathbb{B}) \phi_b(\mathfrak{L}_{\mathbb{B}}) \prod_{(\mathbf{x}, \ell) \in \mathbb{B}} \tilde{b}(\mathbf{x}, \ell), \quad (64)$$

where $\tilde{b}(\mathbf{x}, \ell)$ is the single object birth density corresponding to label ℓ , and $\phi_b(L)$ is the birth weight defined by

$$\phi_b(L) = \prod_{\ell \in \mathcal{B} \setminus L} (1 - r_b(\ell)) \prod_{\ell \in L} 1_{\mathcal{B}}(\ell) r_b(\ell), \quad (65)$$

in which $r_b(\ell)$ is the existence probability of the newborn object with label ℓ .

The overall prediction of the multi-object state at the next time step is the union of survivals and new births, i.e. $\mathbb{X}_+ | \mathbb{X} = \mathbb{S} \cup \mathbb{B}$. The label spaces \mathcal{L} and \mathcal{B} are disjoint, and the states of newborn objects are independent of surviving objects, hence \mathbb{S} and \mathbb{B} are independent. It can be shown [64] that the multi-object transition can be expressed as a product of the transition density for surviving objects and the density of newborn objects:

$$\tilde{\Pi}(\mathbb{X}_+ | \mathbb{X}) = \tilde{\Pi}_S(\mathbb{X}_+ \cap (\mathcal{X} \times \mathcal{L}) | \mathbb{X}) \cdot \tilde{f}_b(\mathbb{X}_+ \setminus (\mathcal{X} \times \mathcal{L})). \quad (66)$$

Both the GLMB and δ -GLMB families are closed under the Chapman-Kolmogorov prediction with this transition [64].

6.3. δ -GLMB particle filter

Suppose that the posterior multi-object density at time $k - 1$ is a δ -GLMB with the label space \mathcal{L} , given by (61), i.e.

$$\tilde{f}_{k-1}(\mathbb{X}) = \Delta(\mathbb{X}) \sum_{(I, \xi) \in \mathcal{F}(\mathcal{L}) \times \Xi} \phi_{k-1}^{I, \xi} \delta[I, \mathfrak{L}_{\mathbb{X}}] \prod_{(\mathbf{x}, \ell) \in \mathbb{X}} \tilde{p}_{k-1}^{\xi}(\mathbf{x}, \ell) \quad (67)$$

in which the distribution $\tilde{p}_{k-1}^{\xi}(\mathbf{x}, \ell)$ of the target with label ℓ and measurement association history ξ is represented by a weighted set of particles

$$\{w_{k-1}^{(i), \xi}(\ell), \mathbf{x}_{k-1}^{(i), \xi}(\ell)\}_{1 \leq i \leq N_{\ell}^{\xi}}.$$

The particle weights are normalised, i.e. $\sum_{i=1}^{N_{\ell}^{\xi}} w_{k-1}^{(i), \xi}(\ell) = 1$ and we can write:

$$\tilde{p}^{\xi}(\mathbf{x}, \ell) \approx \sum_{i=1}^{N_{\ell}^{\xi}} w_{k-1}^{(i), \xi}(\ell) \delta(\mathbf{x} - \mathbf{x}_{k-1}^{(i), \xi}(\ell)). \quad (68)$$

The goal of the δ -GLMB particle filter is to recursively compute the posterior δ -GLMB density, conditioned on new sets of measurements as they are received.

As usual this is done by first applying the Chapman-Kolmogorov equation with the multi-object transition model, which yields the predicted δ -GLMB density at the next observation time k . Bayes rule is then applied to this prediction using the multi-object likelihood model and the received measurement set. The result is the posterior δ -GLMB density at time k . The prediction and update steps are described next.

Prediction

Let us assume that within the LMB birth model (64), the single-object density $\tilde{b}(\mathbf{x}, \ell)$ corresponding to the target with label ℓ is approximated by particles $\{w_b^{(i)}(\ell), \mathbf{x}_b^{(i)}(\ell)\}_{1 \leq i \leq N_\ell^b}$. Under the labelled multi-object transition model defined in (66), the predicted multi-object density at time k is a δ -GLMB with the label space $\mathcal{L}_+ = \mathcal{L} \cup \mathcal{B}$, given by [64]

$$\tilde{f}_{k|k-1}(\mathbb{X}) = \Delta(\mathbb{X}) \sum_{(I_+, \xi) \in \mathcal{F}(\mathcal{L}_+) \times \Xi} \phi_+^{I_+, \xi} \delta[I_+, \mathfrak{L}_{\mathbb{X}}] \prod_{(\mathbf{x}, \ell) \in \mathbb{X}} \tilde{p}_+^\xi(\mathbf{x}, \ell), \quad (69)$$

where, assuming the bootstrap-type particle filter with the importance density equal the (single-target) transitional density,

$$\phi_+^{I_+, \xi}(L) = \phi_b(I_+ \cap \mathcal{B}) \cdot \phi_s^\xi(I_+ \cap \mathcal{L}), \quad (70)$$

$$\tilde{p}_+^\xi(\mathbf{x}, \ell) \approx \begin{cases} \sum_{i=1}^{N_\ell^\xi} w_s^{(i), \xi}(\ell) \delta(\mathbf{x} - \mathbf{x}_s^{(i), \xi}(\ell)), & \text{if } \ell \in \mathcal{L} \\ \sum_{i=1}^{N_\ell^b} w_b^{(i)}(\ell) \delta(\mathbf{x} - \mathbf{x}_b^{(i)}(\ell)), & \text{if } \ell \in \mathcal{B} \end{cases} \quad (71)$$

$$\mathbf{x}_s^{(i), \xi}(\ell) \sim \pi_{k|k-1}(\mathbf{x} | \mathbf{x}_{k-1}^{(i), \xi}(\ell)), \quad i = 1, \dots, N_\ell^\xi \quad (72)$$

$$w_s^{(i), \xi}(\ell) \propto w_{k-1}^{(i), \xi}(\ell) \tilde{p}_s(\mathbf{x}_{k-1}^{(i), \xi}(\ell), \ell), \quad i = 1, \dots, N_\ell^\xi \quad (73)$$

$$\eta_s^\xi(\ell) = \sum_{i=1}^{N_\ell^\xi} w_{k-1}^{(i), \xi}(\ell) \tilde{p}_s(\mathbf{x}_{k-1}^{(i), \xi}(\ell), \ell), \quad (74)$$

$$\phi_s^\xi(M) = \left(\prod_{\ell \in M} \eta_s^\xi(\ell) \right) \sum_{I \subseteq \mathcal{L}} 1_I(M) \phi_{k-1}^\xi(I) \prod_{\ell \in I \setminus M} [1 - \eta_s^\xi(\ell)]. \quad (75)$$

In principle, the δ -GLMB prediction involves generating a new predicted component (hypothesis) for every combination of target birth, death and survival, for each component in the current posterior density. In practice however, doing so is usually infeasible because the number of combinations becomes prohibitively large. To improve the efficiency, approximations can be made that avoid computing unlikely components. One approach is to use a “shortest paths” algorithm to generate the most likely combinations of targets.

This can be carried out separately for births and survivals, using the graph structures shown in Fig. 4. Each row in the graphs in Fig. 4 corresponds to a target label: the left-hand column represents target survival/birth, and the right-hand column represents target death/non-birth. The goal is to maximise the predicted component weights, which are expressed in (70), (75) and (65) as products of single-target weights. Since the shortest paths algorithm is based on minimising a set of additive path costs, negative logarithms are used to change the problem from maximum-product to minimum-sum form. Paths are generated from top-to-bottom, and only those targets corresponding to rows in which the left-hand column was visited are included in the prediction.

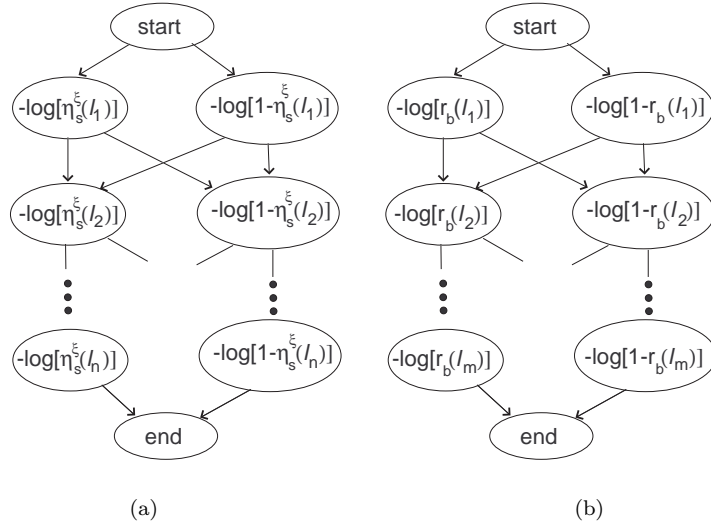


Figure 4: Graph structures for δ -GLMB prediction: (a) survival prediction graph; (b) birth prediction graph. Note that the labels in (a) and (b) are disjoint sets.

Pseudo-code of the prediction step of the δ -GLMB particle filter is given in Alg. 6. The input to this function in line 2 represents $\tilde{f}_{k-1}(\mathbb{X})$ of (67), with L_{k-1}^h being the set of target labels according to hypothesis $h = 1, \dots, H$. The input also includes the number of predicted components to be generated for each component in the current density, that is K^h for $h = 1, \dots, H$. The input in line 3 represents $\tilde{f}_b(\mathbb{B})$ of (64). Note that the **ShortestPaths** function returns a collection of pairs $\{(L^j, c^j)\}_{1 \leq j \leq K}$, where each L^j is a list of surviving target labels, and c^j is the corresponding path cost (the negative logarithm of the

weight).

Algorithm 6 The prediction step of the δ -GLMB particle filter

```

1: function  $\delta$ -GLMB PARTICLE FILTER: PREDICTION STEP
2:   Input:  $\left\{ L_{k-1}^h, \phi_{k-1}^h, \left\{ \left\{ w_{k-1}^{(i),h}(\ell), \mathbf{x}_{k-1}^{(i),h}(\ell) \right\}_{1 \leq i \leq N_\ell^h} \right\}_{\ell \in L_{k-1}^h}, K^h \right\}_{1 \leq h \leq H_{k-1}}$ 
3:   Input:  $\left\{ r_b(\ell), \left\{ w_b^{(i)}(\ell), \mathbf{x}_b^{(i)}(\ell) \right\}_{1 \leq i \leq N_\ell^b} \right\}_{\ell \in \mathcal{B}}, K_b$ 
4:   Construct graph  $\mathcal{G}_b$  according to Figure 4.(b)
5:    $\left\{ (L_b^j, c_b^j) \right\}_{1 \leq j \leq K_b} = \text{ShortestPaths}(\mathcal{B}, \mathcal{G}_b, K_b)$ 
6:    $m = 1$ 
7:   for  $h = 1, \dots, H_{k-1}$  do
8:     Construct graph  $\mathcal{G}_S^h$  according to Figure 4.(a)
9:      $\left\{ (L_S^{h,j}, c_S^{h,j}) \right\}_{1 \leq j \leq K^h} = \text{ShortestPaths}(L_{k-1}^h, \mathcal{G}_S^h, K^h)$ 
10:    for  $j = 1, \dots, K^h$  do
11:      for  $\beta = 1, \dots, K_b$  do
12:         $L_+^m = L_b^\beta \cup L_S^{h,j}$ 
13:         $\phi_+^m = \phi_{k-1}^h \exp(-c_b^\beta) \exp(-c_S^{h,j})$ 
14:        Compute  $\left\{ w_+^{(i),m}(\ell), \mathbf{x}_+^{(i),m}(\ell) \right\}_{1 \leq i \leq N_+^m(\ell)}, \forall \ell \in L_+^m$  ▷ Eqn (71)
15:         $m = m + 1$ 
16:      end for
17:    end for
18:  end for
19:   $H_+ = m - 1$ 
20:  Normalise weights  $\left\{ \phi_+^j \right\}_{1 \leq j \leq H_+}$ 
21:  Output:  $\left\{ L_+^h, \phi_+^h, \left\{ \left\{ w_+^{(i),h}(\ell), \mathbf{x}_+^{(i),h}(\ell) \right\}_{1 \leq i \leq N_+^h(\ell)} \right\}_{\ell \in L_+^h} \right\}_{1 \leq h \leq H_+}$ 
22: end function

```

Update

The prior multi-object density at time $k - 1$ is a δ -GLMB given by (69) and represented by line 21 of Alg. 6. Next we wish to compute the posterior multi-object density $\tilde{f}_{k|k}(\mathbb{X})$, conditioned on a set of received measurements \mathbf{Z}_k .

Let Θ be the set of all mappings of target labels to measurement indices, $\theta : \mathbb{L} \rightarrow \{0, 1, \dots, |Z|\}$, such that $[\theta(i) = \theta(j) > 0] \Rightarrow [i = j]$. Note that a given θ can map multiple labels to 0, meaning that there can be multiple misdetected targets. However, only one label can be mapped to each non-zero measurement index, which means that each measurement can only be assigned to one target. Under the standard multi-object observation likelihood $\varphi_k(\mathbf{Z}|\mathbb{X})$ (see the first paragraph of Sec. 6.2), the posterior multi-object density is a δ -GLMB given

by [64]

$$\tilde{f}_{k|k}(\mathbb{X}) = \Delta(\mathbb{X}) \sum_{(I_+, \xi) \in \mathcal{F}(\mathcal{L}_+) \times \Xi} \sum_{\theta \in \Theta(\Omega_{\mathbb{X}})} \phi_Z^{I_+, \xi, \theta} \delta[I_+, \Omega_{\mathbb{X}}] \prod_{(\mathbf{x}, \ell) \in \mathbb{X}} \tilde{p}^{\xi, \theta}(\mathbf{x}, \ell | \mathbf{Z}_k), \quad (76)$$

where

$$\phi_Z^{I_+, \xi, \theta}(L) = \frac{\phi_+^{I_+, \xi}(L) \prod_{\ell \in I_+} \eta_Z^{\xi, \theta}(\ell)}{\sum_{(J, \alpha) \in \mathcal{F}(\mathcal{L}_+) \times \Xi} \sum_{\theta \in \Theta(J)} \omega^{J, \alpha}(J) \prod_{\ell \in J} \eta_Z^{\alpha, \theta}(\ell)}, \quad (77)$$

$$\tilde{p}^{\xi, \theta}(\mathbf{x}, \ell | \mathbf{Z}) \approx \sum_{i=1}^{N_\ell^\xi} \frac{w_+^{(i), \xi}(\ell) \tilde{\psi}_Z(\mathbf{x}_+^{(i), \xi}(\ell), \ell; \theta)}{\eta_Z^{\xi, \theta}(\ell)} \delta(\mathbf{x} - \mathbf{x}_+^{(i), \xi}(\ell)), \quad (78)$$

$$\eta_Z^{\xi, \theta}(\ell) = \sum_{i=1}^{N_\ell^\xi} w_+^{(i), \xi}(\ell) \tilde{\psi}_Z(\mathbf{x}_+^{(i), \xi}(\ell), \ell; \theta), \quad (79)$$

$$\tilde{\psi}_Z(\mathbf{x}, \ell; \theta) = \begin{cases} \frac{\tilde{p}_D(\mathbf{x}, \ell) g_k(\mathbf{z}_{\theta(\ell)} | \mathbf{x}, \ell)}{\lambda c(\mathbf{z}_{\theta(\ell)})}, & \theta(\ell) > 0 \\ 1 - \tilde{p}_D(\mathbf{x}, \ell), & \theta(\ell) = 0 \end{cases}. \quad (80)$$

In principle, the update involves generating a new δ -GLMB component for all possible associations of measurements to targets. This is not usually feasible in practice, since the number of associations increases combinatorially with the number of targets and measurements. An effective method of reducing the number of posterior δ -GLMB components is to use a ranked assignment algorithm to generate a requested number of components with highest weights. For a set of targets with labels $\{\ell_1, \dots, \ell_n\}$, and a set of measurements $\mathbf{Z} = \{\mathbf{z}_1, \dots, \mathbf{z}_m\}$, this can be achieved by constructing the following cost matrix,

$$-\log \begin{pmatrix} \vartheta^\xi(\ell_1, \mathbf{z}_1) & \cdots & \vartheta^\xi(\ell_1, \mathbf{z}_m) & \vartheta^\xi(\ell_1, \emptyset) & \cdots & 0 \\ \vdots & \ddots & \vdots & \vdots & \ddots & \vdots \\ \vartheta^\xi(\ell_n, \mathbf{z}_1) & \cdots & \vartheta^\xi(\ell_n, \mathbf{z}_m) & 0 & \cdots & \vartheta^\xi(\ell_n, \emptyset) \end{pmatrix}, \quad (81)$$

where

$$\vartheta^\xi(\ell, \mathbf{z}) = \sum_{i=1}^{N_\ell^\xi} \frac{w_+^{(i), \xi}(\ell) \tilde{p}_D(\mathbf{x}_+^{(i), \xi}(\ell)) g_k(\mathbf{z} | \mathbf{x}_+^{(i), \xi}(\ell))}{\lambda c(\mathbf{z})} \quad (82)$$

$$\vartheta^\xi(\ell, \emptyset) = \sum_{i=1}^{N_\ell^\xi} w_+^{(i), \xi}(\ell) (1 - \tilde{p}_D(\mathbf{x}_+^{(i), \xi}(\ell))) \quad (83)$$

In (81), each row represents a target, the first m columns represent detections, and the last n columns represent misdetections. Note that if measurement gating is carried out beforehand, many of the detection terms in the first m columns will be zero, indicating that the corresponding measurement-to-target association is infeasible. The matrix (81) is processed using a ranked assignment algorithm. For example, Murty's algorithm [68], yields a sorted list of the cheapest one-to-one assignments of rows to columns, in increasing order of cost. Note that using this formulation, each solution must assign every row to a column, but there may be columns that are not assigned to a row. In generating the list of ranked assignments, whenever a row is assigned to a column index greater than m by Murty's algorithm, the assignment is reported as 0, to indicate that the target was misdetected. Each element in the list is then used to construct a component in the posterior δ -GLMB density.

Pseudo-code for the δ -GLMB particle filter update step is given in Alg. 7. Similarly to the prediction, the input includes the components of the prior δ -GLMB, and the number of posterior components M^h for $h = 1, \dots, H_+$ to generate for each prior component.

Estimation of labelled target states

The final step in the filtering recursion is to estimate the labelled target states based on the posterior δ -GLMB density. One method is to approximate the posterior δ -GLMB in the form of a labelled multi-Bernoulli PDF, where each target label has an associated existence probability. Assuming the posterior δ -GLMB density is specified by line 24 in Alg. 7, for each $\ell \in \cup_{m=1}^{H_k} L_k^m$ the existence probability is computed as

$$r_{k,\ell} = \sum_{m=1}^{H_k} \phi_k^m 1_{L_k^m}(\ell). \quad (84)$$

The corresponding spatial PDF $p_{k,\ell}(\mathbf{x})$ is approximated by a weighted particle set obtained as a union:

$$\cup_{m=1}^{H_k} \begin{cases} \emptyset, & \text{if } \ell \notin L_k^m \\ \left\{ \phi_k^m \cdot w_k^{(i),m}(\ell), \mathbf{x}_k^{(i),m}(\ell) \right\}_{1 \leq i \leq N_\ell^m}, & \text{if } \ell \in L_k^m \end{cases}$$

A threshold can then be applied to $r_{k,\ell}$ to determine which tracks are to be reported.

A simpler alternative method, which we use here, is to first compute the

Algorithm 7 The update step of the δ -GLMB particle filter

```

1: function  $\delta$ -GLMB PARTICLE FILTER UPDATE
2:   Input:  $\mathbf{Z}_k, \left\{ L_+^h, \phi_+^h, \left\{ \left\{ w_+^{(i),h}(\ell), \mathbf{x}_+^{(i),h}(\ell) \right\}_{1 \leq i \leq N_+^h(\ell)} \right\}_{\ell \in L_+^h}, M^h \right\}_{1 \leq h \leq H_+}$ 
3:    $m = 1$ 
4:   for  $h = 1, \dots, H_+$  do
5:     Compute the cost matrix  $C_Z^h$  according to (81)
6:      $\{(\theta^{h,j}, c^{h,j})\}_{1 \leq j \leq M^h} = \text{RankedAssignments}(L_+^h, C_Z^h, M^h)$ 
7:     for  $j = 1, \dots, M^h$  do
8:        $L_k^m = L_+^h$ 
9:        $\phi_k^m = \phi_+^h \exp(-c^{h,j})$ 
10:      for  $\ell \in L_k^m$  do
11:         $\tilde{\mathbf{x}}_k^{(i),m}(\ell) = \mathbf{x}_+^{(i),h}(\ell), \quad i = 1, \dots, N_+^h(\ell)$ 
12:         $\tilde{w}_k^{(i),m}(\ell) = w_+^{(i),h}(\ell) \tilde{\psi}_Z(\mathbf{x}_+^{(i),h}(\ell), \ell; \theta^{h,j}), \quad i = 1, \dots, N_+^h(\ell)$ 
13:         $w_k^{(i),m}(\ell) = \tilde{w}_k^{(i),m}(\ell) / \sum_{j=1}^{N_+^h(\ell)} \tilde{w}_k^{(j),m}(\ell) \quad \triangleright \text{(Normalisation)}$ 
14:        for  $i = 1, \dots, N_\ell^h$  do  $\triangleright \text{(Resampling)}$ 
15:          Select index  $j^i \in \{1, \dots, N_+^h(\ell)\}$  with probability  $w_k^{(i),m}(\ell)$ 
16:           $\mathbf{x}_k^{(i),m}(\ell) = \tilde{\mathbf{x}}_k^{(j^i),m}(\ell)$ 
17:        end for
18:      end for
19:       $m = m + 1$ 
20:    end for
21:  end for
22:   $H_k = m - 1$ 
23:  Normalise weights  $\{\phi_k^m\}_{1 \leq m \leq H_k}$ 
24:  Output:  $\left\{ L_k^m, \phi_k^m, \left\{ \left\{ w_k^{(i),m}(\ell), \mathbf{x}_k^{(i),m}(\ell) \right\}_{1 \leq i \leq N_\ell^m} \right\}_{\ell \in L_k^m} \right\}_{1 \leq m \leq H_k}$ 
25: end function

```

posterior cardinality distribution of the δ -GLMB as follows:

$$\rho(n) = \sum_{m=1}^{H_k} \phi_k^m \cdot \delta[n, |L_k^m|], \quad n = 0, 1, 2, \dots$$

The maximum a posteriori estimate of the target cardinality is then

$$\hat{n} = \arg \max_n [\rho(n)].$$

The next step is to select a component m^* as the highest weighted δ -GLMB component representing cardinality \hat{n} . The set of reported target states consist of the labels and weighted particle sets in the component m^* .

6.4. Demonstration: Bearings-only multi-object tracking

The performance of the described δ -GLMB particle filter is demonstrated by application to bearings-only multi-target tracking. The scenario geometry and parameters are the same as those used in Sec. 5.4. The δ -GLMB filter retains the top 100 hypotheses after each scan, and uses 5000 particles per target. The number of hypotheses generated in the prediction is 1000, and the number generated in the update is 4000. A single run output tracks of the δ -GLMB particle filter are shown in Fig. 5. The ground truth tracks are shown by thick solid lines (compare with Fig. 3.a), while the estimated tracks are represented by the same coloured thin lines. Because all four targets in the scenario are moving from left to right, the accuracy of estimated tracks also improves from left to right.

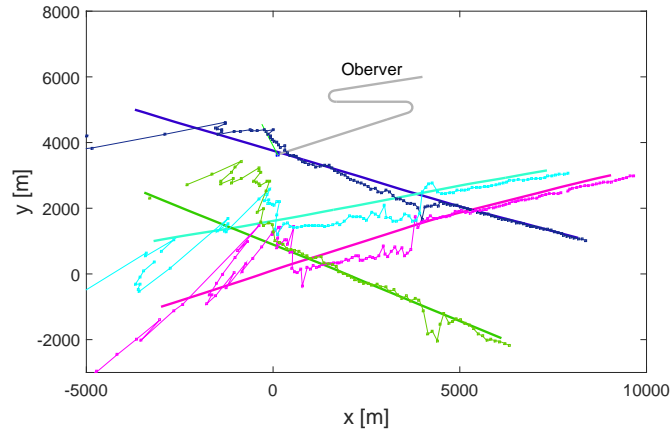


Figure 5: A single run of the δ -GLMB particle filter applied to bearings-only multi-target tracking.

The average tracking performance is studied next. For comparison sake, we also present the tracking results of the Bernoulli particle filter (Sec. 4.3) which has been modified to track multiple targets via the use of the “linear multi-target” (LM) technique proposed in [69]. The LM technique is an approximation in which the detections from the nearby targets are considered as false detections that affect only the clutter density $c(\mathbf{z})$. This filter is referred to as the LM-Bernoulli particle filter. Fig. 6 shows the mean OSPA errors, obtained by averaging over 500 Monte Carlo runs of the δ -GLMB PF and the LM-Bernoulli PF. One can observe that the average performance of the two tracking filters is almost equivalent when the targets are well separated. However, when the

targets approach each other (from around 1400s to 1900s), the δ -GLMB PF exhibits better performance. This is to be expected since the δ -GLMB PF is an implementation of the principled Bayes-optimal multi-target tracker. We can also comment on the performance of the two Bernoulli-type tracking particle filters versus the PHD particle filters, whose OSPA errors were shown in Fig. 3.(b). First, recall that the tracking filters produce tracks (as opposed to the PHD filters, which produce only multi-target state estimates). Comparing Figs. 3 and 6 we also observe that both Bernoulli-type tracking particle filters achieve somewhat lower mean OSPA errors than the PHD particle filter described in Sec. 5.

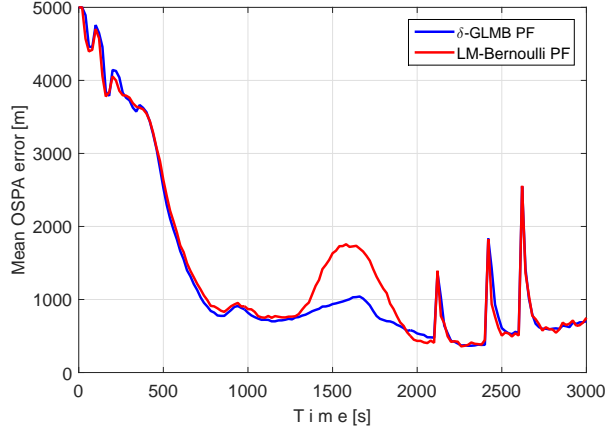


Figure 6: Bearings-only multi-target tracking results: the mean OSPA error of the δ -GLMB particle filter (blue) and the LM-Bernoulli particle filter (red).

7. Summary and further reading

This overview paper is an attempt to describe the particle method based implementation of the new class of Bayes-optimal and suboptimal filters, derived using random finite set models. The primary focus was on the Bernoulli PF, the probability hypothesis density PF and the δ -generalised labelled multi-Bernoulli PF. Each of these particle filters has been studied in detail and subsequently demonstrated in the context of bearings-only filtering/tracking.

Particle filters for random finite set models is a growing research field and there are many topics that this overview paper could not address due to the space limitation. For an interested reader we briefly list some of these topics: different (non-standard) measurement models (e.g. intensity measurements

[70], [71], extended versus point target measurements [72],[73],[74],[75], group tracking [76], finite sensor resolution or merged measurements [77], [78],[26]); multi-sensor fusion aspects [79]; smoothing (as opposed to filtering) [80]; sensor control aspects [35] and handling the switching dynamic models [81].

References

- [1] A. H. Jazwinski. *Stochastic processes and filtering theory*. Academic press, 1970.
- [2] A. Doucet, J. F. G. de Freitas, and N. J. Gordon, editors. *Sequential Monte Carlo Methods in Practice*. Springer, 2001.
- [3] M. S. Arulampalam, S. Maskell, N. Gordon, and T. Clapp. A tutorial on particle filters for non-linear/non-Gaussian Bayesian tracking. *IEEE Trans. Signal Processing*, 50(2):174–188, Feb. 2002.
- [4] P. Djuric, J. H. Kotecha, J. Zhang, Y. Huang, T. Ghirmai, M. Bugallo, and J. Miguez. Particle filtering. *IEEE Signal Processing Magazine*, pages 19–38, Sept. 2003.
- [5] B. Ristic, S. Arulampalam, and N. Gordon. *Beyond the Kalman filter: Particle filters for tracking applications*. Artech House, 2004.
- [6] O. Cappé, S. J. Godsill, and E. Moulines. An overview of existing methods and recent advances in sequential Monte Carlo. *Proc. IEEE*, 95(5):899–924, 2007.
- [7] A. Doucet and A. M. Johansen. A tutorial on particle filtering and smoothing: Fifteen years later. *Handbook of Nonlinear Filtering*, 12:656–704, 2009.
- [8] S. M. Kay. Fundamentals of statistical signal processing, Vol. II: Detection theory. *Prentice Hall*, 1998.
- [9] R. P. S. Mahler. *Advances in Statistical Multisource-multitarget information fusion*. Artech House, 2014.
- [10] Y. Bar-Shalom, X. R. Li, and T. Kirubarajan. *Estimation with Applications to Tracking and Navigation*. John Wiley & Sons, 2001.
- [11] S. J. Julier and J. K. Uhlmann. Unscented filtering and nonlinear estimation. *Proceedings of the IEEE*, 92(3):401–422, 2004.
- [12] S. Challa, M. R. Morelande, D. Mušicki, and R. J. Evans. *Fundamentals of Object Tracking*. Cambridge Univ. Press, 2011.
- [13] C. P. Robert and G. Casella. *Monte Carlo statistical methods*. Springer, 2nd edition, 2004.

- [14] C. Berzuini and W. R. Gilks. Resample-move filtering with cross-model jumps. In A. Doucet, N. De Freitas, and N. Gordon, editors, *Sequential Monte Carlo Methods in Practice*, chapter 6. Springer, 2001.
- [15] N. J. Gordon, D. J. Salmond, and A. F. M. Smith. Novel approach to nonlinear/non-Gaussian Bayesian state estimation. *IEE Proc.-F*, 140(2):107–113, 1993.
- [16] A. Doucet, S. Godsill, and C. Andrieu. On sequential Monte Carlo sampling methods for Bayesian filtering. *Statistics and Computing*, 10(3):197–208, 2000.
- [17] M. Pitt and N. Shephard. Filtering via simulation: Auxiliary particle filters. *Journal of the American Statistical Association*, 94(446):590–599, 1999.
- [18] R. Van der Merwe, A. Doucet, N. De Freitas, and E. Wan. The unscented particle filter. In *Advances in Neural Information Processing Systems*, volume 13. 2000.
- [19] F. Daum, J. Huang, and A. Noushin. Exact particle flow for nonlinear filters. In *Proc. SPIE*, volume 7697, 2010.
- [20] C. Musso, N. Oudjane, and F. LeGland. Improving regularised particle filters. In A. Doucet, N. deFreitas, and N. J. Gordon, editors, *Sequential Monte Carlo methods in Practice*. Springer, 2001.
- [21] P. B. Quang, C. Musso, and F. Le Gland. Particle filtering and the laplace method for target tracking. *IEEE Trans. Aerospace and Electronic Systems*, 2015. (to appear).
- [22] B. W. Silverman. *Density estimation for statistical and data analysis*. Chapman and Hall, 1986.
- [23] C. Andrieu, A. Doucet, and R. Holenstein. Particle Markov chain Monte Carlo methods. *Journ. Royal Statistical Soc. B*, 72(Part 3):269–342, 2010.
- [24] T. Schon, F. Gustafsson, and P. J. Nordlund. Marginalized particle filters for mixed linear/nonlinear state-space models. *IEEE Trans Signal Processing*, 53(7):2279–2289, 2005.
- [25] S. Arulampalam, M. Clark, and R. Vinter. Performance of the shifted Rayleigh filter in single-sensor bearings-only tracking. In *Proc. 10th IEEE Int. Conf. Information Fusion*, July 2007.
- [26] M. Beard, B.-T. Vo, and B.-N. Vo. Bayesian multi-target tracking with merged measurements using labelled random finite sets. *IEEE Trans. Signal Processing*, 63(6):1433–1447, 2015.

- [27] R. Mahler. *Statistical Multisource Multitarget Information Fusion*. Artech House, 2007.
- [28] B. N. Vo, S. Singh, and A. Doucet. Sequential Monte Carlo methods for multi-target filtering with random finite sets. *IEEE Trans. Aerospace & Electronic Systems*, 41(4):1224–1245, Oct. 2005.
- [29] B. Ristic, B.-T. Vo, B.-N. Vo, and A. Farina. A tutorial on Bernoulli filters: Theory, implementation and applications. *IEEE Trans. Signal Processing*, 61(13):3406–3430, 2013.
- [30] B. Ristic. *Particle filters for random set models*. Springer, 2013.
- [31] Y. Boers and J. N. Driessen. A particle filter multi target track before detect application. *IEE Proc. Radar, Sonar and Navigation*, 151(6):351–357, 2004.
- [32] H. Sidenbladh and S. L. Wirkander. Tracking random sets of vehicles in terrain. In *Proc. 2nd IEEE Workshop on Multi-Object Tracking*, Madison, WI, USA, June 2003.
- [33] T. Zajic and R. Mahler. A particle-systems implementation of the PHD multi-target tracking filter. In *Proc. SPIE*, volume 5096, pages 291–299, April 2003.
- [34] M. Vihola. Rao-Blackwellised particle filtering in random set multitarget tracking. *IEEE Trans. Aerospace & Electronic Systems*, 43(2):689–705, 2007.
- [35] B. Ristic and B.-N. Vo. Sensor control for multi-object state-space estimation using random finite sets. *Automatica*, 46:1812–1818, 2010.
- [36] S. Reuter and K. Dietmayer. Pedestrian tracking using random finite sets. In *Proc. Int. Conf. Information Fusion*, Chicago, USA, July 2011.
- [37] Y. Boers, E. Sviestins, and H. Driessen. Mixed labelling in multitarget particle filtering. *IEEE Trans Aerospace and Electronic Systems*, 46(2):792–802, 2010.
- [38] R. P. S. Mahler. Multi-target Bayes filtering via first-order multi-target moments. *IEEE Trans. Aerospace & Electronic Systems*, 39(4):1152–1178, 2003.
- [39] M. Tobias and A.D. Lanterman. Probability hypothesis density-based multitarget tracking with bistatic range and Doppler observations. *IEE Proc.-Radar Sonar Navig*, 152(3):195–205, 2005.
- [40] D. Clark, I. T. Ruiz, Y. Petillot, and J. Bell. Particle PHD filter multiple target tracking in sonar image. *IEEE Trans. Aerospace & Electronic Systems*, 43(1):409–416, 2007.

- [41] E. Maggio, M. Taj, and A. Cavallaro. Efficient multitarget visual tracking using random finite sets. *IEEE Trans. Circuits & Systems for Video Technology*, 18(8):1016–1027, 2008.
- [42] C. Lundquist, L. Hammarstrand, and F. Gustafsson. Road intensity based mapping using radar measurements with a probability hypothesis density filter. *IEEE Trans. on Signal Processing*, 59(4):1397–1408, 2011.
- [43] M. Canaud, L. Mihaylova, J. Sau, and N.-E. El Faouzi. Probabilty hypothesis density filtering for real-time traffic state estimation and prediction. *Networks and Heterogeneous Media (NHM)*, 8(3):825–842, 2013.
- [44] J. Mullane, B.-N. Vo, M. D. Adams and B.-T. Vo. A Random-Finite-Set Approach to Bayesian SLAM. *IEEE Transactions on Robotics*, 27(2):268–282, 2011.
- [45] M. Adams, B.-N. Vo, R. Mahler, and J. Mullane. SLAM gets a PHD: New concepts in map estimation. *IEEE Robotics & Automation Magazine*, 21(2):26–37, 2014.
- [46] C. S. Lee, S. Nagappa, N. Palomeras, D. E. Clark, and J. Salvi. Slam with SC-PHD filters: An underwater vehicle application. *IEEE Robotics & Automation Magazine*, 21(2):38–45, 2014.
- [47] S. H. Rezatofighi, S. Gould, B.-N. Vo, K. Mele, and W. E. Hughes and R. Hartley. A multiple model probability hypothesis density tracker for time-lapse cell microscopy sequences. In *Information Processing in Medical Imaging*, pages 110–122. Springer, 2013.
- [48] R. P. S. Mahler. PHD filters of higher order in target number. *IEEE Trans. Aerospace & Electronic Systems*, 43(4):1523–1543, 2007.
- [49] B. Ristic, D. Clark, B.-N. Vo, and B.-T. Vo. Adaptive target birth intensity for PHD and CPHD filters. *IEEE Trans. on Aerospace and Electronic Systems*, 48(2):1656–1668, 2012.
- [50] N. P. Whiteley, S. S. Singh, and S. J. Godsill. Auxiliary particle implementation of the probability hypothesis density filter. *IEEE Trans. on Aerospace & Electronic Systems*, 46(3):1437–1454, July 2010.
- [51] J. H. Yoon, D. Y. Kim, and K.-Y. Yoon. Efficient importance sampling function design for sequential Monte Carlo PHD filter. *Signal Processing*, 92:2315–2321, 2012.
- [52] T. Li, S. Sun, and T. P. Sattar. High speed sigma-gating SMC-PHD filter. *Signal Processing*, 93:2586–2593, 2013.

- [53] B. Ristic. Efficient update of persistent particles in the SMC-PHD filter. In *Proc. IEEE Int. Conf. Acoustic Speech Signal Processing (ICASSP)*, Brisbane, Australia, 2015.
- [54] D. E. Clark, J. Bell, Y. de Saint-Pern, and Y. Petillot. PHD filter for multi-target tracking in 3D sonar. In *Proc. IEEE OCEANS-05-Europe*, pages 265–270, Brest, France, 2005.
- [55] B. Ristic, D. E. Clark, and N. Gordon. Calibration of multi-atrget tracking algorithms using non-cooperative targets. *IEEE Journal of Selected Topics in Signal Processing*, 7(3):390–398, 2013.
- [56] B. Ristic and D. Clark. Particle filter for joint estimation of multi-object dynamic state and multi-sensor bias. In *Proc. IEEE Int. Conf. Acoustics, Speech & Signal Proc. (ICASSP)*, pages 3877–3880, Kyoto, Japan, March 2012.
- [57] A. Swain and D. E. Clark. First-moment filters for spatial independent cluster processes. *Proc. of SPIE 7697*, 2010.
- [58] A. Swain and D. Clark. Extended object filtering using spatial independent cluster processes. *Proc. Int. Conf. Information Fusion*, 2010.
- [59] C. S. Lee, D. E. Clark, and J. Salvi. SLAM with dynamic targets via single-cluster PHD filtering. *IEEE Journal of Selected Topics in Signal Processing*, 7(3):543–552, 2013.
- [60] D. Schuhmacher, B.-T. Vo, and B.-N. Vo. A consistent metric for performance evaluation of multi-object filters. *IEEE Trans. Signal Processing*, 56(8):3447–3457, 2008.
- [61] L. Lin, Y. bar Shalom, and T. Kirubarajan. Track labelling and PHD filter for multitarget tracking. *IEEE Trans Aerospace and Electronic Systems*, 42(3):778–795, 2006.
- [62] J. Yang and H. Ji. A novel track maintenance algorithm for PHD/CPHD filter. *Signal Processing*, 92:2371–2380, 2012.
- [63] B.-T. Vo, B. N. Vo, and A. Cantoni. The cardinality balanced multi-target multi-Bernoulli filter and its implementations. *IEEE Trans. on Signal Processing*, 57(2):409–423, 2009.
- [64] B.-T. Vo and B.-N. Vo. Labeled random finite sets and multi-object conjugate priors. *IEEE Trans. on Signal Processing*, 61(13):3460–3475, 2013.
- [65] B.-N. Vo, B.-T. Vo, and D. Phung. Labeled random finite sets and the Bayes multi-target tracking filter. *IEEE Trans. on Signal Processing*, 62(24):6554–6567, 2014.

- [66] J. L. Williams. An efficient, variational approximation of the best fitting multi-Bernoulli filter. *IEEE Trans. Signal Processing*, 63(1):258–273, 2015.
- [67] J. Correa, M. Adams, and C. Perez. A Dirac delta mixture-based random finite set filter. *Proc. IEEE Int. Conf. Control, Automation and Information Sciences (ICCAIS)*, 2015.
- [68] K. G. Murty. An algorithm for ranking all the assignments in order of increasing cost. *Operations Research*, 16(3):682–687, 1968.
- [69] D. Musicki and B. La Scala. Multi-target tracking in clutter without measurement assignment. *IEEE Trans. Aerospace and Electronic Systems*, 44(3):877–896, July 2008.
- [70] B.-N. Vo, B.-T. Vo, N.-T. Pham, and D. Suter. Joint detection and estimation of multiple objects from image observations. *IEEE Trans. Signal Processing*, 58(10):5129–5141, 2010.
- [71] F. Papi, B.-N. Vo, B.-T. Vo, C. Fantacci, and M. Beard. Generalized labeled multi-Bernoulli approximation of multi-object densities. *IEEE Trans. Signal Processing*, 63(20):5487–5497, Oct. 2015.
- [72] K. Granström, C. Lundquist, and O. Orguner. Extended target tracking using a Gaussian-mixture PHD filter. *IEEE Trans. on Aerospace and Electronic Systems*, 48(4):3268–3286, 2012.
- [73] B. Ristic and J. Sherrah. Bernoulli filter for joint detection and tracking of an extended object in clutter. *IET Radar, Sonar & Navigation*, 7(1):26–35, 2013.
- [74] Meiqin Liu, Tongyang Jiang, and Senlin Zhang. The sequential Monte Carlo multi-Bernoulli filter for extended targets. In *18th Intern. Conf. on Information Fusion*, pages 984–990, 2015.
- [75] M. Beard, S. Reuter, K. Granström, B.-T. Vo, B.-N. Vo, and A. Scheel. Multiple extended target tracking with labelled random finite sets. *IEEE Trans. Signal Processing*, 2016. In print.
- [76] A. Swain and D. Clark. The single-group PHD filter: an analytic solution. In *Proc. 14th Int. Conf. Information Fusion*, Chicago, USA, July 2011.
- [77] R. Mahler. PHD filters for nonstandard targets, II: unresolved targets. In *Proc. 12th Int. Conf. Information Fusion*, pages 922–929, Seattle, USA, 2009.
- [78] F. Lian, C. Han, W. Liu, J. Liu, and J. Sun. Unified cardinalized probability hypothesis density filters for extended targets and unresolved targets. *Signal Processing*, 92(7):1729–1744, 2012.

- [79] M. Uney, S. Julier, D. Clark, and B. Ristic. Monte carlo realisation of a distributed multi-object fusion algorithm. In *IET Sensor Signal Processing for Defence (SSPD 2010)*, 2010.
- [80] R. P. S. Mahler, B.-T. Vo, and B.-N. Vo. Forward-backward probability hypothesis density smoothing. *IEEE Trans. Aerospace and Electronic Systems*, 48(1):707–728, Jan 2012.
- [81] D. Dunne and T. Kirubarajan. Multiple model multi-Bernoulli filters for manoeuvring targets. *IEEE Trans. Aerospace and Electronic Systems*, 49(4):2679–2692, 2013.